UNIVERSITY OF CALIFORNIA SAN DIEGO

The Subcellular Localization of the Vacuolar-type ATPase in Symbiodiniaceae Algae and Its Potential Role in Supporting Photosynthesis

A Thesis submitted in partial satisfaction of the requirements
for the degree Master of Science

in

Marine Biology

by

Qianqian Tao

Committee in charge:

Professor Martin Tresguerres, Chair
Professor Ronald Burton
Professor Stuart Sandin

2024

The Thesis of Qianqian Tao is approved, and it is acceptable in quality and form for publication on microfilm and electronically.

University of California San Diego

2024

DEDICATION

This thesis is dedicated to my mother and father, Zhaohong Tan and Sheng Tao, whose support and encouragement have always been my greatest source of motivation. Your love, patience, and belief in me have guided me throughout my academic journey. I also want to express my gratitude to my beloved siblings, Peng Tao and Merlyn Tao, for always being my great friends and source of strength. I would like to extend my appreciation to all the members of the Tresguerres lab, who have provided invaluable guidance and support during my time in the lab. Special thanks to my advisor, Dr. Martin Tresguerres, for your patience and mentorship, and to my mentors, Dr. Claudia Tatiana Galindo Martínez, Dr. Alexander Clifford, and Dr. Angus Thies for your unwavering support. To my cohort friends, Bryan Delgado, Elisa Prohroff, and Victoria Vasquez, your valuable friendship has been a cornerstone throughout the program. Lastly, I am deeply grateful to Dr. Ronald Burton and Dr. Stuart Sandin for serving on my thesis committee and aiding me in my research.

TABLE OF CONTENTS

LIST OF FIGURES

LIST OF TABLES

LIST OF ABBREVIATIONS

ATP	Adenosine triphosphate
ATPase	Adenosine triphosphatase
bp	Base pair
BSA	Bovine serum albumin
CA	Carbonic anhydrase
Ca^{+}	Calcium ion
$CaCl_2$	Calcium chloride
CCM	CO_2-concentrating mechanism
cDNA	Complementary deoxyribonucleic acid
CO_2	Carbon dioxide
ConcA	Concanamycin A
CTAB	Cetyltrimethylammonium bromide
DAPI	4′,6-diamidino-2-phenylindole
DCMU	3-(3,4-dichlorophenyl)-1,1-dimethylurea
DIC	Differential interference contrast
DMSO	Dimethylsulfoxide
DNA	Deoxyribonucleic acid
DNase	Deoxyribonuclease
ECL	Enhanced chemiluminescence
EZ	Ethoxzolamide
GAR	Goat anti-rabbit
gDNA	Genomic deoxyribonucleic acid

GFP	Green fluorescent protein
H^+	Proton/hydrogen ion/acid molecule
H_2O	Water
HCO_3^-	Bicarbonate
HRP	Horseradish peroxidase
ICC	Immunocytochemistry
KCl	Potassium chloride
kDA	Kilodalton
KLH	Keyhole limpet hemocyanin
Mg^{2+}	Magnesium ion
$MgCl_2$	Magnesium chloride
mRNA	Messenger ribonucleic acid
NaCl	Sodium chloride
O_2	Oxygen
PBS	Phosphate buffered saline
PBS-TX	Phosphate buffered saline with 0.2% Triton-X
PCR	Polymerase chain reaction
PFA	Paraformaldehyde
PMA	Plasma membrane-type H^+ ATPase
PMCA	Plasma membrane Ca^{2+} ATPase
RNase	Ribonuclease
RPM	Revolutions per minute
RT	Room temperature

Rubisco	Ribulose-1,5-bisphosphate carboxylase/oxygenase
SDS-PAGE	Sodium dodecyl sulfate–polyacrylamide gel electrophoresis
TBS	Tris-buffered saline
TBS-T	Tris-buffered saline with 0.1% Tween 20
UV	Ultraviolet
VHA	Vacuolar-type H^+ ATPase

ACKNOWLEDGEMENTS

This work was funded by UC Scholars, University of California, San Diego to Qianqian Tao and grants from the Gordon and Betty Moore Foundation (Award 9325) and the National Science Foundation (NSF-BSF IOS 2149926) to Martin Tresguerres.

ABSTRACT OF THE THESIS

The Subcellular Localization of the Vacuolar-type ATPase in Symbiodiniaceae Algae and Its Potential Role in Supporting Photosynthesis

by

Qianqian Tao

Master of Science in Marine Biology

University of California San Diego, 2024

Professor Martin Tresguerres, Chair

Host vacuolar-type ATPase (VHA)-mediated carbon-concentrating mechanisms (CCMs) that promote photosynthesis have been observed in coral-, sea anemone-, and giant clam-Symbiodiniaceae symbiosis. Similarly, analogous CCMs operate in some free-living secondary endosymbiotic algae, where VHA is present in phagocytic-origin membranes surrounding the chloroplasts. This thesis explored the potential role of VHA in the CCM of cultured

Symbiodiniaceae algae *Breviolum psygmophilum* and *Miliolidium leei*, which establish symbiosis with corals and foraminifera, respectively. VHA subunit B (VHA_B) transcripts were detected in *B. psygmophilum* and symbiotic algae in the coral *Stylophora pistillata*. *B. psygmophilum* acclimated to 60 and 400 µmol photons m^{-2} s^{-1} contained similar amounts of VHA_B proteins per cell; however, VHA_B constituted a higher proportion of total protein under the high light condition. Respirometry experiments indicated that VHA inhibition decreased O_2 production in *B. psygmophilum* cultures when illuminated by the light level they were acclimated to, suggesting a VHA-mediated CCM under these conditions. However, the effects of pharmacological inhibitors varied across replicates and times, suggesting that the CCM is highly responsive to light level, pH, inorganic carbon concentration, algal circadian rhythm and growth phases. Effects of drug concentration and drug incubation time should also be carefully considered. Unfortunately, *B. psygmophilum* ruptured in the chemical fixative, which prevented establishing the subcellular localization of VHA_B. Successful immunolocalization of VHA_B in *M. leei* that fixed properly revealed that VHA_B surrounded intracellular spherical structures resembling vacuoles but not the chloroplast. These results highlight morphological and physiological differences between these two species within Symbiodiniaceae.

INTRODUCTION

Symbiodiniaceae is a family of photosynthetic secondary endosymbiotic dinoflagellates that can live freely in the seawater column (Fujise et al., 2021; Takabayashi et al., 2012) and can also establish a symbiotic relationship with other organisms (LaJeunesse et al., 2018). In symbiosis, Symbiodinineaceae are found intracellularly in many aquatic invertebrates and protists (LaJeunesse, 2002; Pawlowski et al., 2001) or extracellularly in porifera and some bivalve mollusks (Carlos et al., 1999). They are notable for their ecological function as endosymbionts in reef-building corals from the order Scleractinia, which provide habitat for numerous organisms creating one of the most productive ecosystems on earth (Muscatine and Trench, 1975; Muscatine, 1990; Trench, 1987 & 1993). The symbiotic algae provide essential photosynthates such as glucose and glycerol to their hosts, in some cases providing over 100% of the hosts' carbohydrates, which is key to the evolutionary success of corals in oligotrophic areas (Muscatine et al., 1984; Muscatine, 1990; Trench, 1979). Some coral species acquire symbiotic algae either through vertical transmission from parent to offspring via eggs or as brooded larvae (Baird et al., 2009), while others acquire them horizontally from the environment (Abrego et al., 2009; Harrison & Wallace, 1990). The alga that enters the coral gastrovascular cavity is engulfed by gastrodermal cells by phagocytosis and maintained within an intracellular compartment known as the symbiosome. The symbiosome membrane mediates all metabolic exchanges between the host cell and the symbiotic algae. The metabolism of the symbionts is believed to be closely regulated by the microenvironment within the symbiosome, which is then controlled by the coral host (Barrot et al., 2015; Thies et al., 2022; Wooldridge, 2010).

In all eukaryotic cells, phagocytosis is mediated by the conserved Vacuolar-type H^+ ATPase (VHA). VHA has a cytosolic V1 domain for the hydrolysis of ATP, which energizes the

translocation of H^+ across biological membranes against electrochemical gradients through its V0 domain (Forgac, 2007). This function enables VHA to drive acidification in phagosomes during phagocytosis, aiding in the destruction of ingested microorganisms (Di et al., 2006). However, when algae are engulfed by the host cell, they are not digested but instead maintained in symbiosis. Reflecting the link between phagocytosis and coral-algae symbiosis, the symbiosome membrane can contain abundant VHA and this enzyme can significantly acidify the symbiosome space. This acidification favors the partitioning of CO_2 over HCO_3^- as part of a carbon concentrating mechanism (CCM) around the symbiotic algae, which promotes photosynthesis (Barott et al., 2015). A similar VHA-dependent host-controlled CCM has also been observed in sea anemones and giant clams hosting symbiotic Symbiodinineaceae algae intracellularly and extracellularly, respectively, which implies a conserved mechanism for host control of photosynthesis across two invertebrate phyla–Cnidaria and Mollusca (Armstrong et al., 2018; Barott et al., 2022)

VHA and CO_2-concentrating mechanism in microalgae

A further link between phagocytosis and photosynthesis via VHA is observed in some free-living secondary endosymbiotic algae such as diatoms (Yee et al 2023). It has been shown that VHA located on the two additional eukaryotic-origin membranes surrounding the chloroplasts contributes to the algal CCM. Secondary endosymbiosis originated from a process that took place after the primary endosymbiosis events that resulted in eukaryotic cells with mitochondria and chloroplasts. Secondary endosymbiosis ensued when a heterotrophic eukaryotic protist engulfed a red alga, which was subsequently reduced to a chloroplast over evolutionary time. As a result of secondary endosymbiosis, the chloroplast is surrounded by additional two membranes of eukaryotic origin membranes: the inner endoplasmic reticulum membrane derived from the red

alga and the outer endoplasmic reticulum membrane from the protist (reviewed by McFadden, 2001). Dinoflagellates have experienced further loss of the red-alga-origin membrane, resulting in a chloroplast with only three membranes (Lee, 1977). Given its eukaryotic origin and enzymatic activity, VHA is believed to be present in these additional membranes and acidifies compartments in the chloroplast, thereby concentrating CO_2 around ribulose-1,5-bisphosphate carboxylase/oxygenase (RuBisCO) and promoting photosynthesis—a critical component of CCM (Lee & Kugrens, 1998; Lee & Kugrens, 2000).

In photosynthetic organisms, CCM helps compensate for RuBisCO's low affinity for CO_2. RuBisCO is a key enzyme that catalyzes the initial step of carbon fixation in the Calvin-Benson-Bassham cycle of the light-independent reaction. It originated in the Archaean Eon in an O_2-free atmosphere, where CO_2 levels were approximately 50 times higher than they are today (Berner, 2006). Following the emergence of photosynthetic organisms in the early Proterozoic era, the levels of atmospheric O_2 began to rise while CO_2 concentrations decreased (Canfield, 2005). This change in the atmospheric CO_2 to O_2 ratio adversely affected RuBisCO's efficiency in CO_2 fixation, since it has a dual functionality as a carboxylase/oxygenase and O_2 increasingly competes with CO_2 to proceed with photorespiration that impairs CO_2 fixation and consumes fixed CO_2 (Andrews & George, 1987). However, the modern atmospheric CO_2 levels are far below RuBisCO's half-saturation point, and thus most photosynthetic organisms have developed CCMs that elevate the concentration of CO_2 at the site of RuBisCO. However, the molecular mechanisms can vary between Phyla and habitat. For example, the diffusion rate of CO_2 in water is slower than in air, and its increased conversion into HCO_3^- in neutral or alkaline pH further exacerbates the catalytic limitations of RuBisCO in aquatic ecosystems. CCMs in microalgae usually involve membrane transporting proteins to take up HCO_3^- from the surrounding water and carbonic anhydrase (CA)

enzymes that reversibly dehydrate HCO_3^- and H^+ into CO_2, which concentrates CO_2 around RuBisCO and promotes photosynthesis (Pronina & Semenenko, 1990; Pronina, Ramazanov & Semenenko, 1981).

Experiments with transgenic *Thalassiosira pseudonana* diatoms expressing eGFP-VHA_B confirmed VHA's essential role in CCM and photosynthesis (Yee et al., 2023). Confocal imaging revealed that VHA encircled the chloroplast, and its inhibition using the macrolide antibiotic Concanamycin A (ConcA) led to reduced carbon fixation, particularly under conditions of low light and low dissolved inorganic carbon levels (Yee et al., 2023). Additionally, VHA inhibition resulted in decreased O_2 reduction in secondary endosymbiotic algae such as the centric diatom *Thalassiosira pseudonana*, the pennate diatom *Phaeodactylum tricornutum*, the dinoflagellate *Brandtodinium nutricula*, and the coccolithophore *Emiliania huxleyi*, whereas it had no effect in primary endosymbiotic algae like the green alga *Chlorella protothecoides* and the red alga *Porphyrydium purpurneum.* These findings support the hypothesis that VHA is situated in the two eukaryotic-origin membranes surrounding the chloroplasts of secondary endosymbiotic algae and likely enhances their photosynthetic efficiency (Yee et al., 2023).

Given that VHA has been reported to participate in the CCM of various free-living secondary endosymbiotic algae including two diatoms, one dinoflagellate of the genus *Brandtodinium*, and one coccolithophore (Yee et al., 2023), I hypothesized that free-living Symbiodiniaceae algae may employ a similar VHA-mediated CCM. However, symbiotic Symbiodiniaceae algae likely utilize a different mechanism, as they benefit from the host's symbiosomal VHA-dependent CCM (Barott et al., 2015). In addition, an algae-specific type IIIa plasma membrane-type H^+-ATPase (PMA) was expressed in symbiotic algae but not in their free-living counterparts (Bertucci et al., 2010). Although functional data is lacking, it was hypothesized

that PMA may assist in acidifying the symbiosome, thereby enhancing algal photosynthesis (Bertucci et al., 2010). Interestingly, VHA inhibition only partially decreased symbiosomal acidification short term (Barrott et al 2015), suggesting the existence of additional acidifying mechanisms that may include PMA. Moreover, transcriptomic studies have shown differences in gene regulation between symbiotic and free-living algae, with findings regarding the differential expression of VHA and PMA in various Symbiodiniaceae species (Baumgarten et al., 2013; Nedeljka Rosic, 2015; Tingting Xiang et al., 2015). Further investigation into the conditions that trigger the regulation of these two genes is crucial for understanding their roles in the algae.

In addition to mediating phagocytosis and CCM, VHA has been found to play several other critical roles: it promotes silica cell wall biomineralization during cell division in diatoms (Yee et al., 2020), couples with Ca^{2+} channels to generate bioluminescence in dinoflagellates (Kwok et al., 2023), and controls autophagy, which affects lipid production and accumulation in diatoms (Couso et al., 2018; Zhang et al., 2016). Given the involvement of VHA in multiple processes, PCR and western blotting can determine its mRNA expression and protein abundance in algae but cannot identify its subcellular localization or potential roles in CCM. To answer these questions, immunocytochemistry (ICC) and measurement of photosynthetic parameters such as O_2 production rate and carbon fixation rate should be included.

In this thesis, I explored the role of VHA in the CCM of cultured Symbiodiniaceae algae *Breviolum psygmophilum* and *Miliolidium leei*. These two species can establish symbiosis with corals and foraminifera, respectively. To achieve my goals, I compared VHA subunit B (VHA_B) mRNA expression in *B. psygmophilum* and in the coral *Stylophora pistillata* hosting *Symbiodinium sp.* (Clade A) and assessed VHA_B protein abundance in *B. psygmophilum* cultures acclimated to low (60 µmol photons m^{-2} s^{-1}) and high (400 µmol photons m^{-2} s^{-1}) light levels. I also evaluated

VHA's role on photosynthesis under varying light conditions by measuring O_2 production in *B. psygmophilum* with and without the VHA inhibitor, Concanamycin A. However, I had trouble fixing *B. psymophilum* for ICC as the cells ruptured in the chemical fixatives, so I moved on using *M. leei* that fixed well in the chemical fixatives and examined the subcellular localization of VHA_B in *M. leei.* Unfortunately, *M. leei* cultures grow very slowly which precluded obtaining enough material for respirometry experiments. Nevertheless, these findings reaffirm great morphology and physiology diversity within the Symbiodiniaceae family.

MATERIALS AND METHODS

Algae Culture and Coral

Symbiodiniaceae algae *Breviolum psygmophilum* (Mf10.14b, Clade B) were originally isolated from stony coral *Orbicella faveolata* (Buffalo Undersea Reef Research collections). *Miliolidium leei* (RT401, Clade D) were originally isolated from foraminifera *Amphisorus hemprichii* (Pochon & LaJeunesse, 2021). These two algae were cultured in 20 ml glass vials containing 12 ml of ASP-8A media with a pH around 8.2 to 8.5 (MCLAUGHLIN & ZAHL, 1966) with antibiotics (Ampicillin 100 ug/ml, Kanamycin 50 ug/ml, Penicillin 50 u/ml and Streptomycin 50 ug/ml) (ASP-8A+α) under continuous light of 90 µmol photons m^{-2} s^{-1} at 25°C with a 12:12-h light:dark cycle. For the O_2 respirometry experiment, cultures were acclimated to either the low light level 60 µmol photons m^{-2} s^{-1} (LL) or the high light level 400 µmol photons m^{-2} s^{-1} (HL) for at least 1 month prior to the experiment. Coral *Stylophora pistillata* containing *Symbiodinium sp.* (Clade A) were grown in flow-through seawater at 26ºC exposed to 70 µmol photons m^{-2} s^{-1}. Coral fragments were sampled during the light period for all experiments.

DNA and RNA Extraction

The protocol for coral holobiont DNA extraction was modified from this Plant DNA Isolation using Phenol/Chloroform Extraction protocol (OPS Diagnostics; Readington, NJ). Four coral fragments ~ 2 cm in length were cut from the coral colony and washed in filtered seawater and Ca^{2+}-Mg^{2+}-free artificial seawater. The coral fragments were then cut into smaller pieces to maximize surface area and put into a 50 ml Falcon tube with 10 ml of Ca^{2+}-Mg^{2+}-free artificial seawater containing 3% antibiotics-antimycotics and penicillin-streptomycin solution (Thermo

Fisher Scientific; Waltham, MA). The tube was attached to a rotator above a shaking incubator (120 RPM) and incubated at 25ºC for 1 h~3 h. After incubation, the mixture was filtered through a 40 µm Nylon Mesh to separate the dissociated coral cells from the skeleton and other debris. The filtered solution containing coral cells was centrifuged at 500 g for 10 min at room temperature (RT). The cell pellet was frozen in liquid nitrogen and quickly thawed. Cetyltrimethylammonium bromide (CTAB) Extraction Solution (TEKNOVA Company; Hollister, CA) was added to the thawed cell pellet (5:1 v:m) and cells were disrupted in sterile glass beads using a bead beater (Benchmark Scientific; Sayreville, NJ) (4 x 15s with a speed of 3 m/s). RNA was removed by addition of 5 ul of 10 mg/ml RNase A (Macherey-Nagel Company; Düren, Germany) and incubation for 15 min at RT. DNA was extracted by adding an equal amount of chloroform: isoamyl alcohol (24:1) and 0.7 volume of isopropanol. The DNA that was extracted in isopropanol were incubated at -80 ºC overnight and centrifuged at 10,000g for 10 min for the formation of the pellet the next day. The pellet was washed 2 times in 75% ethanol and resuspended in 50 µl of TE buffer for DNA. The concentration and quality of the extracted DNA was measured in a NanoDrop® ND-1000 UV-vis spectrophotometer (NanoDrop Technologies; Wilmington, DE).

Coral holobiont RNA was extracted using TRIzol® Reagent (Invitrogen; Waltham, MA) following the manufacturer's instructions. 1 g of coral fragment was ground into powder using mortar and pestle in liquid nitrogen and dissolved in 10 ml of TRIzol® Reagent. The sample was transferred into a glass set of homogenizer pestle and mortar and homogenized up and down on ice for 3 times. The sample was then centrifuged for 10 min at 12,000g (4ºC) to remove the skeleton. 2 ml of chloroform was added to the supernatant, followed by vortexing 15s and incubating 10 min at RT. After a centrifugation (15 min, 12,000×g, 4°C), the solution was separated into a lower phenol-chloroform containing protein, an interphase containing DNA, and

a colorless upper aqueous phase containing RNA. This aqueous phase containing only RNA was transferred to a clean tube. 5 ml of isopropanol was added to the tube, followed by mixing and incubating overnight at -80ºC. After being removed from the fridge, the sample was incubated for 10 min at RT and a centrifugation (10 min, 12,000×g, 4°C) allowed for the formation of the RNA pellet. The pellet was washed 2 times in 75% ethanol and resuspended in 20 µl DNase-RNase-free water (Eppendorf; Hamburg, Germany). Extracted RNA were immediately purified using the RNA purification protocol from the PureLink™ RNA Mini Kit (Thermo Fisher Scientific; Waltham, MA) before cDNA synthesis. The concentration and quality of the extracted RNA was measured in the NanoDrop machine.

The coral holobiont DNA CTAB extraction protocol detailed above was used to extract DNA and RNA from algae culture with the following modifications. 20 ml of algal-cell-containing medium (10^7 cells) was centrifuged at 3,000g for 10 min at RT. The pellet was fast-freezed in liquid nitrogen and resuspended in CTAB solution (5:1 v:m). To obtain RNA, 5 ul of 10 mg/ml DNase (RNase-Free DNase Set, Qiagen; Hilden, Germany) was added to the solution to remove DNA.

PCR

First-strand complementary DNA (cDNA) was synthesized from 1µg of RNA with 50µM Oligo $d(T)_{20}$ primers using the Superscript™ IV First-Strand Synthesis System (Invitrogen; Waltham, MA). Primer sets for genes PMA, RuBisCO and Plasma-membrane Ca^{2+}-ATPase (PMCA) were obtained from Bertucci et al. (2010). The VHA subunit B (VHA_B) primer set was designed by the author and constructed by Integrated DNA Technologies, Inc. (San Diego, USA). PMA, RuBisCO and VHA primers are specific to algae, while PMCA primers are specific to corals

(Table 1). PCR was performed using *Taq* DNA Polymerase (M0267, ThermoPol® Buffer, New England Biolabs; Ipswich, MA), and the reaction conditions were as follow: the initial denaturation was conducted at 95ºC for 30s followed by 33 cycles of denaturation at 95°C for 15 seconds, annealing at 48-57°C for 30 seconds, and elongation at 68°C for 1 minute; the final elongation was done at 68°C for 5 minutes. PCR products were examined using 2% agarose gel electrophoresis in SYBR™ Safe staining (Invitrogen; Waltham, MA) under the UV light. A DirectLoad™ PCR 100 bp low ladder (Sigma-Aldrich; St. Louis, MO) was used to estimate the sizes of the bands. Bands that appeared at approximately the same sizes as predicted were cut and recovered using the Zymoclean™ Gel DNA Recovery Kit (Zymo Research; Tustin, CA). The recovered DNA samples were sequenced and confirmed by Sanger sequencing (Retrogen, Inc.; San Diego, CA).

Table 1. Primer sets information for PCR

Gene	Primer Sets	Annealing Temperature, ºC	Amplicon (bp)
PMA	F:5′-GACGCCCGCTGATGTGGAGTGG-3′ R:5′-GCACCAGGACAATGATGATGCC-3′	57	700 or 320
RuBisCO	F:5′-ACCGGCGTGGGCAAGCTGTTCTCT-3′ R:5′-TGGGAGTGGTCTGCTTCATG-3′	55	433
PMCA	F:5′-ACCATGGCAGAACCTTCAATTAA-3′ R:5′-CCATCGATCCAGCCAGTGTTGTCT-3′	51	438
VHA_B	F:5′-TACTTCGCGTACACGCGCGA-3′ R:5′-GATCTGTCTGTTGTGCAGGG-3′	48	546 or 316

Antibodies

Custom-made rabbit polyclonal anti-VHA_B (PPv3) primary antibodies (Genscript USA, Inc.; Piscataway, NJ) were used for Western blotting and immunocytochemistry. The antigenic epitope sequence is shown in Figure 1. Secondary antibody Goat-Anti-Rabbit horseradish

peroxidase (GAR-HRP) (Bio-Rad; Hercules, CA) was used in western blot. Secondary antibody Goat-Anti-Rabbit 488 (GAR488) was obtained from Thermo Fisher Scientific (Waltham, MA) and used in immunocytochemistry.

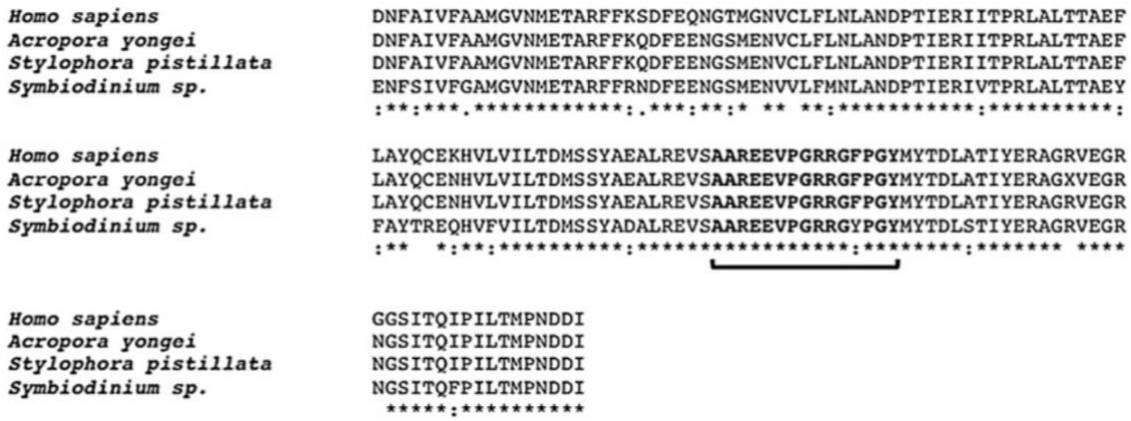

Figure 1. Alignment of the human VHA_B protein sequence with the predicted protein sequences from *Acropora yongei*, *Stylophora pistillata* and *Symbiodinium sp.* A2 (taken from Barott et al., 2015). The epitope of the anti-VHA_B antibody PPv3 is underlined. This region is highly conserved across species.

Western Blot

Algae cultures (1 mL) incubated in DMSO from the O_2 measurement experiment testing 50 nM ConcA were centrifuged at 3000 g for 10 min and immediately stored in -80°C before processing. On the day of western blot, the pellet was resuspended in 100 ul of S22 homogenization buffer [450mM NaCl, 10mM KCl, 58mM $MgCl_2$, 10mM $CaCl_2$, pH 7.6] with 1X Protease Inhibitor Cocktail (Sigma-Aldrich; St. Louis, MO) and 1X PhosStop solution (Roche; Basel, Switzerland), and lysed by sonication (4 times for 15 s). The lysed samples were centrifuged at 500 g for 15 min at 4°C to remove whole cells. The supernatants were transferred to a new tube. Protein concentrations of the supernatants were determined using the Bradford Assay with a BSA

standard curve. The samples were incubated in a 4X Laemmli Sample buffer with 10% β-mercaptoethanol for 15 min at 70 °C and loaded on an SDS-PAGE gel. The amount of samples loaded were either standardized by protein concentration or cell number measured from a haemocytometer. Following gel separation, proteins were transferred to a polyvinylidene difluoride membrane. The membrane was blocked for 1 h on a microplate shaker in blocking buffer I [Tris-buffered saline with 0.1% Tween 20 (TBS-T) and 10% powdered skim milk] at RT, and subsequently incubated overnight at 4 °C with PPv3 antibodies (1:200) in blocking buffer I. The membrane was then washed three times in TBS-T for 10 min each, then stained with the secondary antibodies GAR-HRP. 1:5,000 in blocking buffer I for 1 h at RT on a microplate shaker. The membrane was washed again in TBS-T three times. Bands on the membrane were visualized using the ECL Prime Western Blot Detection Reagent (GE Healthcare, Waukesha, WI) and then imaged with a BioRad Chemidoc Imaging system (Hercules, CA).

O_2 Respirometry Measurements

B. psygmophilum acclimated to LL and HL were harvested at the exponential growth phase. Cell cultures were washed in fresh ASP-8A+α once and then cell concentrations were determined using a hemocytometer. Cell cultures were pre-incubated in DMSO or one of the drugs–concanamycin A (ConcA, 10 nM - 100 nM in DMSO), ethoxzolamide (EZ, 200 nM - 50 µM in DMSO) and 3-(3,4-dichlorophenyl)-1,1-dimethylurea (DCMU, 10 µM) –for either 10 min or 2 h in the dark. O_2 production was measured using an OX-MR O_2 sensor (Unisense; Aarhus, Denmark) in a glass chamber holding 1 ml of culture (1~2 $x10^6$ of cells) at 25 °C with a magnet stirring bar. A typical trial includes 5 min dark incubation, 5 min illumination at 60 µmol photons m^{-2} s^{-1}, 5

min illumination at 400 µmol photons m^{-2} s^{-1} and 3 min dark incubation. Net O_2 production rate was measured by calculating the slope of O_2 concentration over the last 2 mins during the 5-min illumination. Respiration rate was calculated similarly over 1 min immediately after illumination. The interaction between factors light illumination during the measurement (60 vs. 400 µmol photons m^{-2} s^{-1}) and drugs (DMSO vs. ConcA or EZ or DCMU) for each light acclimation was analyzed by two-way repeated measures analysis of variance (ANOVA) tests in R Studio (Version 2023.12.1+402) using the package "rstatix". A p-value < 0.05 is denoted by "*", < 0.01 "**" and < 0.001 "***". Paired t-tests were also conducted in R Studio.

Immunocytochemistry

B. psygmophilum and *M. leei* cell cultures (10^7 cells) were centrifuged at 500g at RT for 10 min to a pellet, which was washed with fresh ASP-8A+α media once and resuspended in 1 ml of 4% Paraformaldehyde (PFA) solution (32% stock diluted in ASP-8A+α). Fixation was performed in a rotator at RT for 1 hour. After fixation, the cells were washed with phosphate-buffered saline (PBS) (pH 7.5) three times and resuspended in 50 uL of PBS. However, *B. psygmophilum* ruptured after fixation and only *M. leei* cells were used for the following procedures. Originally, the 5uL of fixed cells were loaded on glass slides using 20 ul of Poly-D-Lysine (Thermo Fisher Scientific, Waltham, MA). A hydro-barrier was drawn around the sample followed by incubation in phosphate-buffered saline with 0.2% Triton-X (PBS-TX) for 10 min. Then, the sample was incubated in blocking buffer II [4 ml PBS-Tx, 80 µl normal goat serum, and 0.8 µl keyhole limpet hemocyanin] in a humidified chamber for 1 h at RT on a microplate shaker (120 RPM). The samples were incubated in a humid chamber on a microplate shaker in all the following steps

before imaging. The blocking buffer was removed, and primary antibodies diluted in blocking buffer II (1:200 PPv3) were added to the sample. No primary control was incubated in PBS. The slides were incubated overnight at 4 °C. The samples were washed in 1X PBS-TX for 3 times 5 min each, and secondary antibodies (GAR488) and DAPI (both diluted 1:500 in blocking buffer II) were then added. The samples were washed in 1X PBS-TX for 3 times 5 min each and mounted onto a depressed glass slide fitted with a glass coverslip prior to microscopy imaging. However, no VHA_B signals were observed inside the cell following this method. I then added a freeze-fracture step in liquid nitrogen after fixation detailed in Castillo-Medina et al. (2011). Nevertheless, confocal images still showed no VHA_B signals inside the cell. I then modified a protein immunolocalization protocol typically used in animal tissues including corals described in Barott & Tresguerres (2015) with the following changes. The cells were fixed in the same condition detailed above. After washing in PBS for three times, instead of resuspending in PBS, the cell pellet was dehydrated, embedded in paraffin wax, sectioned in 7 um slices using a microtome, placed onto glass slides and rehydrated according to the protocol. After rehydration including 10 min in PBS-TX, a hydro barrier was drawn around the sample, followed by incubation in the same blocking buffer, primary antibody and secondary antibody described above.

Confocal Imaging

Confocal imaging was conducted using a Zeiss LSM800 inverted confocal microscope equipped with a Zeiss LD LCI Plan-Apochromat 40x/1.2 l mm Korr DIC M27 objective and Zeiss ZEN 2.6 blue edition software (Cambridge, United Kingdom). The following channels were used for imaging: VHA (excitation 488 nm with 1% laser power, detection 400–555 nm), Chlorophyll

A (excitation 561 & 640 nm at 4% & 1% laser power, detection 650–700 nm), and DAPI (excitation 405 nm at 0.15% laser power, detection 400–605 nm).

RESULTS AND DISCUSSION

Gene and protein expression in cultured and symbiotic algae

Figure 2 shows the PCR results of gDNA and cDNA extracted from the coral holobiont *Stylophora pistillata* and *B. psgmophilum*. Bands were excised and sequenced using Sanger sequencing to verify the amplification of target genes. All four genes were detected in the coral holobiont gDNA and cDNA, which includes coral and algal genetic materials. Compared to RuBisCO mRNA, symbiotic algae expressed VHA_B transcripts at a very low level: VHA_B cDNA was detected by PCR only when 4 times the amount of materials were added (Supplemental Figure 1). PCR amplified RuBisCO, PMA and VHA_B genes in *B. psgmophilum* gDNA. The primers that targeted coral PMCA yielded a band ~ 1000 bp. The sequencing result of this 1000-bp band turned out to be fragments of *Homo sapiens* immunoglobulin mRNA, which might be the result of human genomic material contamination during RNA extraction or sequencing procedures. The VHA_B and PMA primers were designed to include introns, enabling differentiation between gDNA and cDNA: PMA gDNA was around 700 bp while the cDNA was around 300 bp; VHA_B gDNA was around 500 bp while the cDNA was around 300 bp. VHA_B cDNA was detected in both symbiotic and *B. psygmophilum* algae, suggesting roles in algal physiology under both conditions. In contrast, PMA cDNA was exclusively detected in the coral holobiont, implying that the coded protein might only be present and functional in symbiosis but not in cultured algae. However, mRNA transcript levels do not necessarily correlate with protein abundances since processes including protein synthesis delay, regulation of protein autophagy, mRNA translation rate modulate protein abundances (reviewed by Liu et al., 2016).

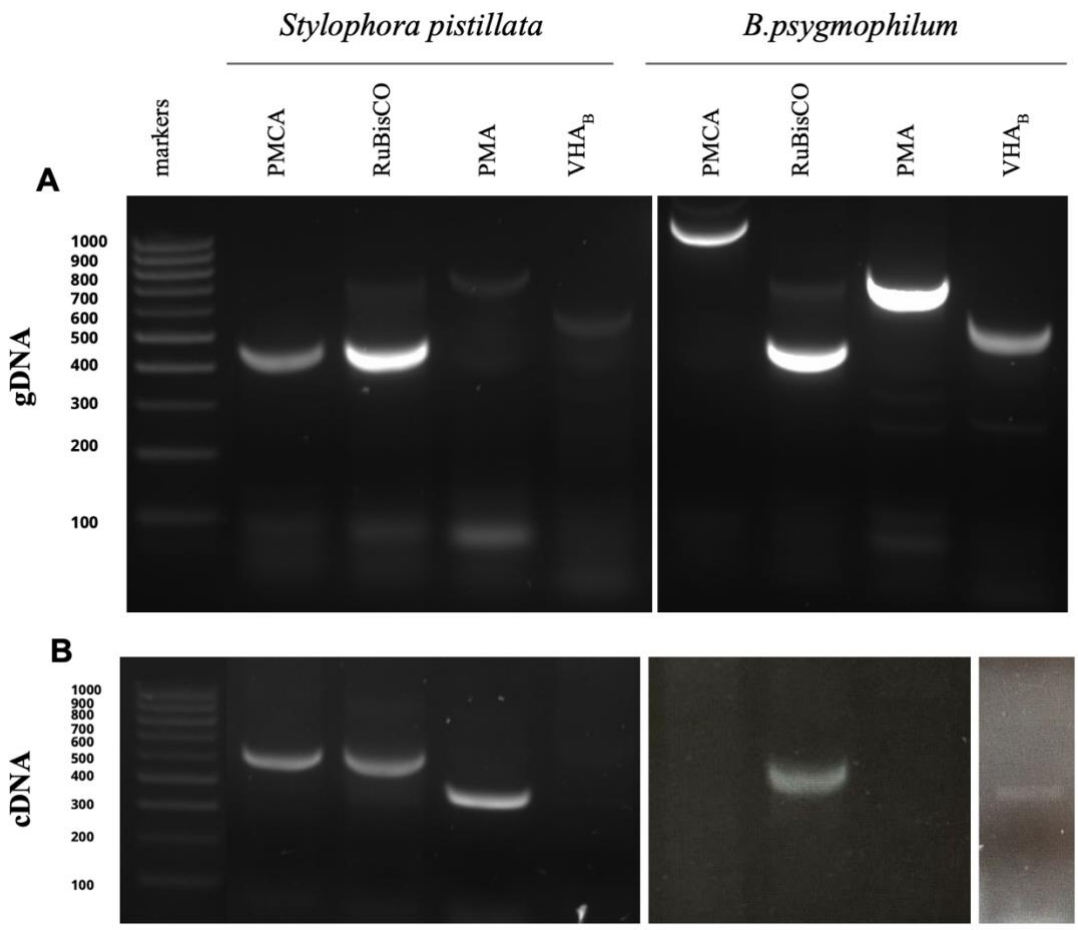

Figure 2. Gene presence and mRNA expression in the coral holobiont *Stylophora pistillata* and *B. psygmophilum* using the primer set listed in Table 1. (A) PCR of the coral holobiont and *B. psygmophilum* gDNA. (B) PCR of the coral holobiont and *B. psygmophilum* cDNA.

Bertucci et al (2010) reported PMA cDNA in the coral *Stylophora pistillata* hosting *Symbiodinium sp.* (Clade A) but not in the same algae in culture, which matches the results from my thesis as well as those reported from cultured algae *Symbiodinium sp.* (Clade A), *Breviolum sp.* (Clade B), *Cladocopium sp.* (Clade C), and *Milliodinium sp.* (Clade D) using RNA-seq (Rosci et al 2015). Though we worked with *B. psygmophilum* (Clade B), sequencing confirmed that the PMA amplicon was PMA. However, other studies have detected PMA transcripts in cultured Symbiodiniaceae algae. A blast search using the 320 bp PMA cDNA sequence against the

Transcriptome Shotgun Assembly database identified PMA transcripts through RNA-seq in *Symbiodinium microadriaticum* (Clade A) originally isolated from *Stylophora pistillata* (Baumgarten et al., 2013) and *Breviolum minutum* (Clade B) (Xiang et al., 2015). And Xiang et al reported similar PMA mRNA expression in cultured and symbiotic *B. minutum* (2015). Since RNA-seq can be more sensitive than end-point PCR (Zhong et al., 2009), it is possible that cultured algae express PMA mRNA at levels too low for detection by end-point-PCR. PMA is encoded by a multigene family and is crucial for various plant physiological processes, including powering H^+/sucrose cotransport in phloem loading and solute uptake in roots (reviewed by Palmgren, 2001). To further understand PMA's function in Symbiodiniaceae algae, future experiments could manipulate nutrient concentrations (e.g., sucrose) or pH and monitor whether PMA transcript level is upregulated under these conditions using qPCR or RNA-seq, or conduct PMA gene knockout experiments to observe phenotypic changes. These experiments could provide insights into its differential roles in symbiosis, particularly in transporting photosynthates to the host and regulating intracellular pH within the acidic symbiosome. This approach might also resolve discrepancies noted in studies like Xiang et al. (2015), by revealing what environmental conditions have influenced PMA transcripts levels.

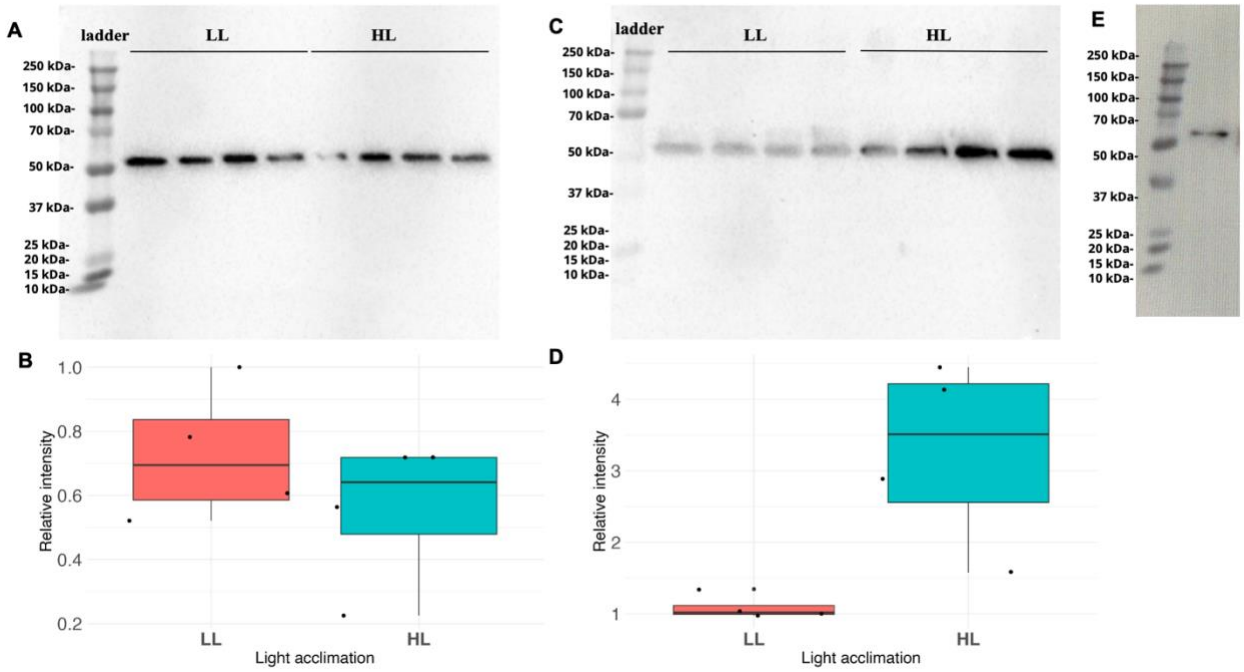

Figure 3. Western blot detection of VHA_B in *B. psygmophilum* and *M. leei*. (A) VHA_B protein production in *B. psygmophilum* acclimated to LL and HL standardized by cell number; proteins extracted from $2.8x10^5$ cells were loaded in each lane. (B) Box plot showing relative band intensity values from blot A (paired t-test, p-value: 0.4643). (C) VHA_B protein production in *B. psygmophilum* acclimated to LL and HL standardized by protein concentration; 4.2 ug of protein were loaded in each lane. (D) Box plot showing relative band intensity values from blot C (paired t-test, p-value: 0.03851 *). (E) Western blot detection of VHA_B in *M. leei* under LL.

Western blot results confirmed the presence of VHA_B protein in both *B. psymophilum* and *M. leei* at the predicted molecular weight of ~ 55 kDa and quantified VHA_B protein abundance in *B. psygmophilum* acclimated to LL and HL (Figure 3). When equivalent amounts of cells were used for western blotting, algae acclimated to LL and HL had similar amounts of VHA_B protein (Figure 3 A & B; p-value = 0.4643 > 0.05). However, when equivalent amounts of protein were loaded, HL algae contained more VHA_B protein compared to LL algae (Figure 3 C & D; p-value = 0.03851 < 0.05 *). Coomassie stained western blot membranes confirm that similar amounts of proteins were loaded to each lane (Supplemental Figure 2). These findings indicate that although

cells acclimated to either light level produced a similar amount of VHA_B proteins, VHA_B constituted a higher proportion of total protein under the high light condition. In other words, HL algae did not upregulate the production of VHA_B proteins but downregulated the production of other proteins. This could be explained, for example, by decreased abundance of photosystem II proteins at HL. Indeed, the abundance of the primary PSII reaction center protein, D1, is known to decrease under high light (600 µmol photons m^{-2} s^{-1}) in *Symbiodinium microadriaticum* (Clade A1 & A1.1), *Symbiodinium bermudense* (Clade B1) and *Fugacium kawagutii* (Clade F2) (Robison & Warner, 2006). Other studies reported upregulation of VHA proteins in the green algae *Chlorella vulgaris* growing under high light (850 µmol photons m^{-2} s^{-1}) compared to low light (70 µmol photons m^{-2} s^{-1}) (Cecchin et al., 2023) and in the marine diatom *Thalassiosira pseudonana* under high light (800 µmol photons m^{-2} s^{-1}) (Dong et al., 2016). However, *C. vulgaris* is a primary endosymbiotic alga that is different from secondary endosymbiotic Symbiodiniaceae algae, and the light levels used in these studies were higher than my HL treatment.

VHA and CA inhibition had various effects on O_2 production of *B. psygmophilum*

Figures 4 and 5 show the O_2 production of *B. psygmophilum* acclimated to LL or HL after 10 min dark incubation in DMSO or 100 nM ConcA or 50 µM EZ. 100 nM ConcA and 50 µM EZ data were compared to the same set of DMSO data. The LL and HL acclimation levels match sub- and super-saturating light levels for Symbiodiniaceae photosynthesis (Iglesias-Prieto & Trench 1994). In LL and HL cultures, net O_2 production rate was higher when illuminated by 400 µmol photons m^{-2} s^{-1}. The only two deviations from this pattern were the LL cultures in DMSO (paired t-test between DMSO treated LL cultures illuminated by 60 and 400 µmol photons m^{-2} s^{-1}; p-value = 0.005 **) and EZ (paired t-test between EZ treated LL cultures illuminated by 60 and 400 µmol

photons m^{-2} s^{-1}; p-value = 0.039 *), which might be due to photoinhibition during 400 µmol photons m^{-2} s^{-1} illumination. All LL cultures produced O_2 at a rate faster than HL cultures when illuminated by 60 µmol photons m^{-2} s^{-1}, but no significant difference between LL and HL cultures was observed when illuminated by 400 µmol photons m^{-2} s^{-1}. In *Symbiodinium microadriaticum* (Clade A), *Fugacium kawagutti* (Clade F) and *Symbiodinium pilosum* (Clade A) acclimated to 40 µmol photons m^{-2} s^{-1} and 250 µmol photons m^{-2} s^{-1}, cultures of the first species acclimated to the lower light level always produced O_2 faster than the higher light level when standardized by cell number, but in the latter two species, the higher light level cultures exceeded the lower light level ones from 100 µmol photons m^{-2} s^{-1} and higher (Iglesias-Prieto & Trench, 1994). Further examination into their photosynthesis systems revealed that these three species had different photosynthetic unit characteristics and cellular concentrations of photosynthetic pigments including chlorophyll *a*, *c2* and peridinin (Iglesias-Prieto & Trench, 1994). Future experiments can focus on evaluating the photosynthetic unit characteristics and generating photosynthesis vs. irradiance curves of *B. psygmophilum* acclimated to different light levels. The photosynthesis vs. irradiance curve monitors the evolution of O_2 production, which helps identify a light level when the HL cultures exceed the LL cultures. Information about photosynthetic unit and pigment characteristics can help explain the variations in their photosynthesis rates under high light illumination observed in these Symbiodiniaceae algae. Net O_2 production rate was negative during 60 µmol photons m^{-2} s^{-1} illumination in HL cultures treated with 100nM and 10nM ConcA (Supplemental Figure 3), which implies that the respiration rate exceeded the photosynthesis rate. In contrast, positive net O_2 production rates were recorded in HL cultures treated with 50 nM ConcA (Supplemental Figure 4B) and 2 µM EZ (Supplemental Figure 5B). The variation might not be directly resulted from the drugs but could be attributed to differences in the algal growth

phase, as approximately 1.0 x 10^6 cells were used in the first two conditions and 1.5 ~2.0 x 10^6 cells in the latter two.

Treatment with ConcA did not significantly impact O_2 production in LL and HL *B. psygmophilum*. Initially, the cultures were incubated in 10 nM ConcA for 2 h in the dark, but this condition did not yield significant change in O_2 production compared to the cultures incubated in DMSO (Supplemental Figure 3). In contrast, 10 nM ConcA has been shown to significantly inhibit photosynthesis in other secondary endosymbiotic algae (Yee et al., 2023). I increased the concentration to 50 nM but still did not see a significant reduction (Supplemental Figure 4). Yee et al (2023) revealed that ConcA had a greater effect at lower dissolved inorganic carbon concentration. I then hypothesized that as the algal cells were producing CO_2 during dark incubation, the cells accumulated CO_2 after a long 2h-dark incubation and did not require CCM in full swing. Thus, I shortened the incubation time to 10 min in the dark to avoid CO_2 accumulation from respiration and increased the drug concentration to 100 nM. According to the two-way repeated measures ANOVA tests, 100 nM ConcA did not significantly affect O_2 production in LL and HL *B. psygmophilum* (Table 2). However, the interaction between light illumination and drug was significant (Table 2, light illumination:drug p-value = 0.006 **) in the LL cultures, as shown in ConcA reducing O_2 production during 60 photons m^{-2} s^{-1} illumination but increasing during 400 µmol photons m^{-2} s^{-1} illumination (Figure 4). I also observed that 100 nM ConcA decreased O_2 production in LL cultures illuminated by the lower light level and HL cultures illuminated by the higher light level. The two-way repeated measures ANOVA test on these two conditions reveals that 100 nM ConcA significantly affect O_2 production (Table 3, drug p-value = 0.017 *). These findings imply that VHA-mediated CCM may exist when the cultures are illuminated by the same light level they are acclimated to. Further increase in concentration was avoided to prevent ConcA

from targeting other ATPases: F-type and P-type ATPases. Additionally, since VHA is involved in multiple cellular processes, ConcA that enters the cell may also inhibit other functions that affect O_2 consumption and production. For example, *Symbiodinium sp.* can engage in heterotrophic feeding during nitrogen depletion (Jeong et al., 2012), which may involve VHA-mediated phagocytosis as observed in heterotrophic flagellates during bacterivory (Obiol et al., 2023).

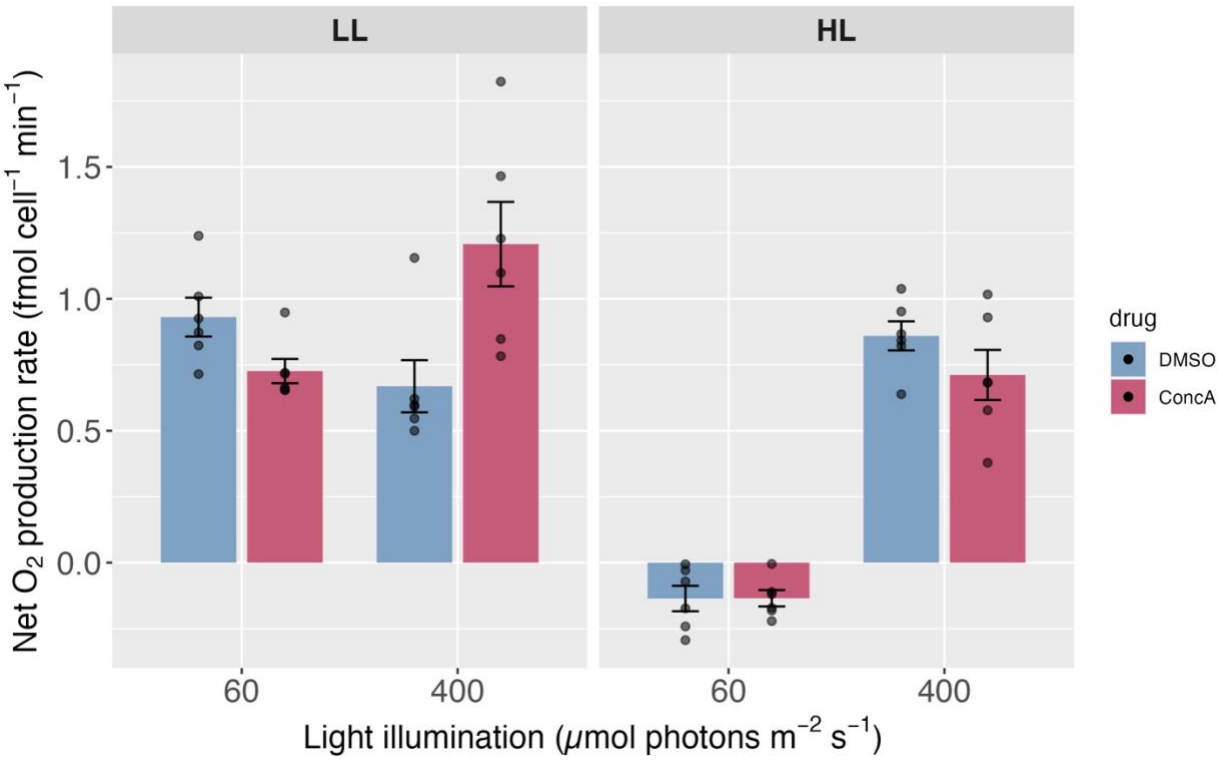

Figure 4. O_2 production of LL (N=6) and HL (N=6) *B. psygmophilum* cultures after 10 min dark incubation in DMSO or 100 nM ConcA.

Table 2. Summary of the two two-way repeated measures ANOVA tests of LL (N=6) and HL (N=6) *B. psygmophilum* algae incubated in DMSO or 100 nM ConcA and illuminated by the two light levels.

	LL P-value	HL P-value
Light illumination	0.186	6.83e-05 ***
Drug	0.080	0.307
Light illumination:drug	0.006 **	0.086

Table 3. Summary of the two-way repeated measures ANOVA test between LL (N=6) *B. psygmophilum* cultures illuminated by 60 µmol photons m^{-2} s^{-1} and HL (N=6) *B. psygmophilum* cultures illuminated by 400 µmol photons m^{-2} s^{-1}. The cultures were incubated in DMSO or 100 nM ConcA.

	P-value
Light illumination	0.462
Drug	0.017 *
Light illumination:drug	0.624

I also tested the carbonic anhydrase inhibitor ethoxzolamide (EZ) in *B. psygmophilum*. As carbonic anhydrase is known to play a role in CCM, inhibiting it should decrease O_2 production. 50 µM of EZ significantly decreased O_2 production in LL *B. psygmophilum* but not in HL cultures (Table 4). However, similar to 100 nM ConcA, 50 µM EZ significantly reduced O_2 production in cultures illuminated by the light level they were acclimated to (Table 5, drug p-value = 0.003 **), which suggests that light levels play an essential role in regulating CCM. The effect of EZ on inhibiting photosynthesis was prominent in many other previous studies. 400 µM of EZ has been

shown to decrease O_2 production by ~80% when the diatom *Phaeodactylum tricornutum* growing under 200 µmol photons m^{-2} s^{-1} was illuminated by 400 µmol photons m^{-2} s^{-1} (Zeng et al., 2019). For *Chlamydomonas reinhardtii* growing under 100 µmol photons m^{-2} s^{-1} when illuminated by 700 µmol photons m^{-2} s^{-1} , 10 nM to 100 µM of EZ has been shown to not significantly affect O_2 production at saturating HCO_3^- level (20 mM) at pH 7.5; while 50 µM of EZ decreased O_2 production by 50% at limiting HCO_3^- level (50 µM) at pH 7.5 and by 30% at pH 5.1 (Moroney et al., 1985).

Respiration rates were not significantly different between DMSO and ConcA treated cultures (Figure 6). EZ did not significantly affect the respiration rate in LL cultures but increased the respiration rate by 35% in HL cultures (Figure 6). However, these respiration rates indicate respiration in the dark but not in the light. The O_2 electrodes I used cannot measure respiration in the light because it can only be measured within the millisecond period after the light is turned off. Therefore, I used net O_2 production rates instead of gross O_2 production rates for the data analysis. DCMU, a drug that inhibits the electron flow from photosystem II to plastoquinone and thus interrupts photosynthesis, was a positive control of this experiment and significantly inhibited photosynthesis (Supplemental Figure 5).

The effect of ConcA and EZ on the O_2 production in *B. psygmophilum* varied greatly in this experiment. I suggest that future researchers carefully choose the light level and drug incubation time when testing these drugs on the O_2 production of photosynthetic organisms. In addition, algal physiological processes including respiration are regulated by algal circadian rhythm. These processes constantly modify the chemical environment including pH and dissolved inorganic carbon concentration surrounding the algae and thus change the photosynthesis rate. Also, cultures in different growth phases, reflected by cell concentrations, were shown to have

different O_2 production rates in this alga. Future researchers should be consistent with the timing of conducting the experiment and the growth phase of the cultures. A high throughput respirometry system would be beneficial in increasing efficiency by enabling simultaneous measurement of multiple samples and different factors.

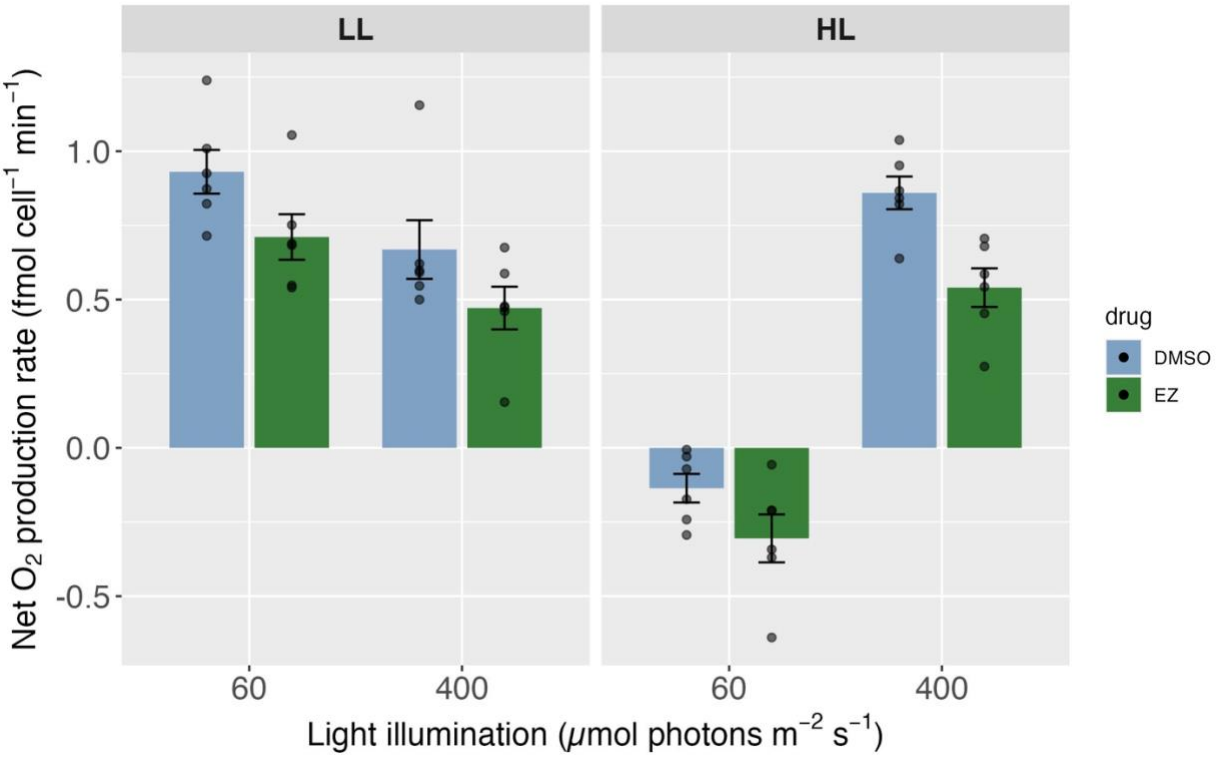

Figure 5. O_2 production of LL (N=6) and HL (N=6) *B. psygmophilum* cultures after 10 min dark incubation in DMSO or 50 µM EZ.

Table 4. Summary of the two two-way repeated measures ANOVA tests of LL (N=6) and HL (N=6) *B. psygmophilum* algae incubated in DMSO or 50 µM EZ and illuminated by the two light levels.

	LL P-value	HL P-value
Light illumination	0.006 **	4.13e-05 ***
Drug	0.143	3.55e-04 ***
Light illumination:drug	0.823	0.044 *

Table 5. Summary of the two-way repeated measures ANOVA test between LL (N=6) *B. psygmophilum* cultures illuminated by 60 µmol photons m^{-2} s^{-1} and HL (N=6) *B. psygmophilum* cultures illuminated by 400 µmol photons m^{-2} s^{-1}. The cultures were incubated in DMSO or 50 µM EZ.

	P-value
Light illumination	0.074
Drug	0.003 **
Light illumination:drug	0.567

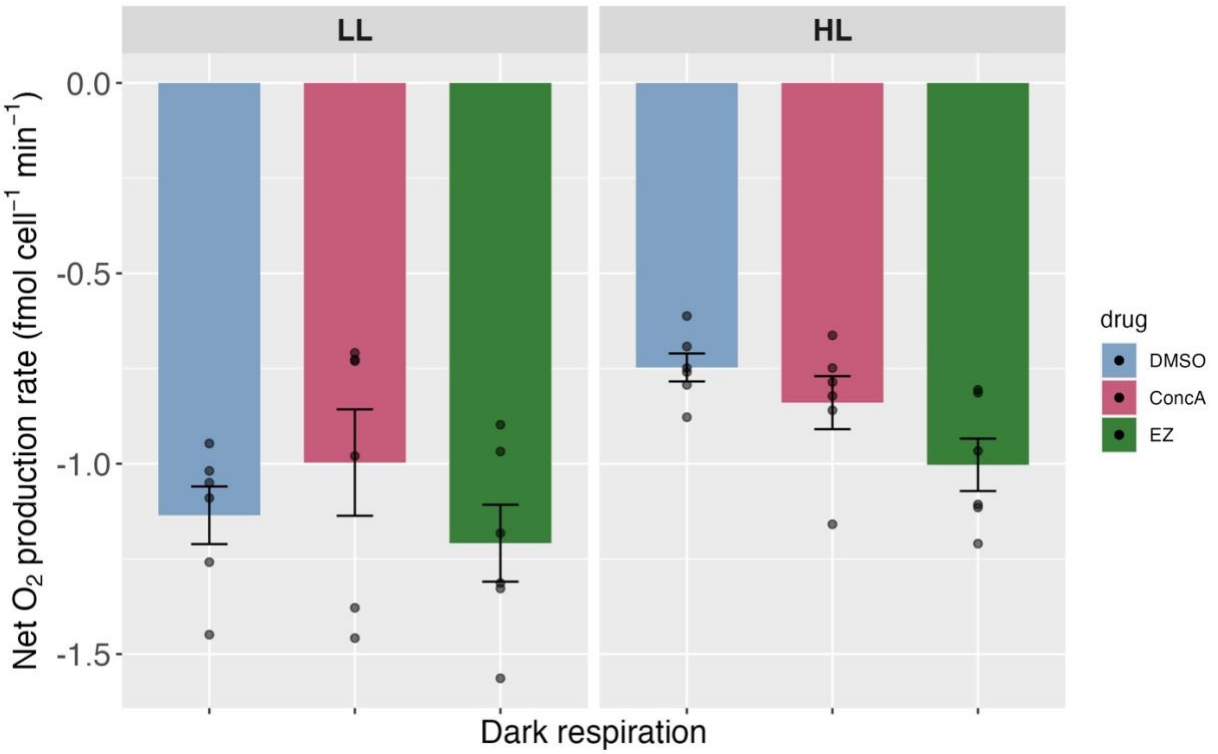

Figure 6. Respiration of LL (N=6) and HL (N=6) *B. psygmophilum* cultures in the dark after incubation in DMSO, 100 nM ConcA or 50 µM EZ. These are the same algae cultures used in Figures 4 & 5.

Differential responses to chemical fixation in the two algae

I initially employed chemical fixation using 4% PFA, but this method resulted in poor fixation of *B. psygmophilum*: a bubble formed in each cell (Figure 7C) and later ruptured (Figure 7D). The chloroplasts in live cells were cup-shaped (Figure 7B). However, the cellular structure was altered after rupture and the chlorophyll A signals became spherical (Figure 7E), which prevents an accurate determination of the original protein subcellular localizations. Despite experimenting with various PFA fixative concentrations (0.01%~32%) and solvent types (seawater, PBS, ASP-8A), cell rupture persisted. I hypothesize that this bubble formation either resulted from

an osmolarity mismatch between the fixative and the cell contents leading to fast water influx or structural changes to the cell wall due to protein cross-linking by the fixative that allowed water to enter. Physical fixation, such as cryofixation that involves fast high-pressure freezing, might be the alternative; however, I was not able to test this method due to time constraints. I shifted my focus to *M. leei* cells, which fixed well using the 4% PFA fixative. The differential responses to chemical fixation between these two algae may be partially attributed to variations in their cell wall compositions, which react differently to PFA. Indeed, different Symbiodiniaceae species can exhibit substantial differences in cellulose content, protein composition, and number of amphiesmal plates in their cell walls (Markell et al., 1992; Tortorelli et al., 2021; Wakefield et al., 2000). However, another issue arose with fixed *M. leei* cells whereby antibodies did not enter the cell, even after trying a freeze-fracture method detailed in Castillo-Medina et al. (2011). Thus, I adapted a protocol typically used in animal tissues including coral (Barott & Tresguerres, 2015). Fixed algal cells were dehydrated and embedded in paraffin wax, which allowed them to be cut into 7 µm slices using a microtome. Given that the algal cells are ~10 µm in diameter, microtome sectioning resulted in cross sections of some cells and exposure of their internal structures to antibodies. This approach was effective, as evidenced by the VHA_B immunofluorescent signal in cells that were sectioned (red arrow) and those that were not (white arrow) and those that had primary antibody and those incubated in PBS control (Figure 8 and Supplemental Figure 6).

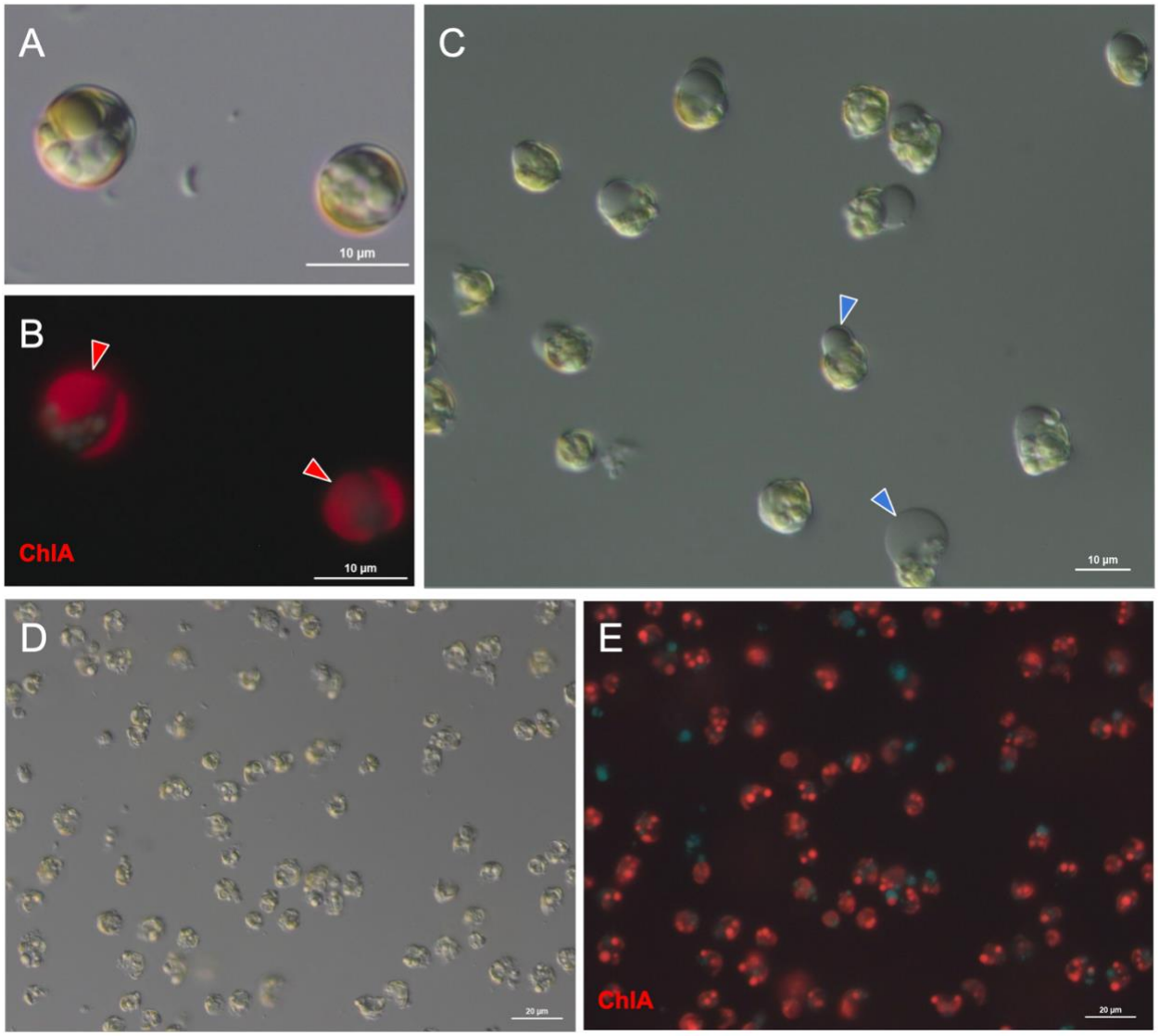

Figure 7. Differential interference contrast (DIC) and fluorescence images of *B. psygmophilum*. (A) DIC image of live cells. (B) Fluorescence image of live cells showing Chlorophyll A signal. The red arrows indicate the location of chloroplasts. (C) Formation of bubbles (indicated by blue arrows) inside cells after 1 hour in 4% PFA at RT. (D) Cell rupture observed after overnight fixation in 4% PFA at RT. (E) Fluorescence image of ruptured cells showing Chlorophyll A signal. ChlA: chlorophyll A.

VHA$_B$ surrounds spherical structures in *M. leei*

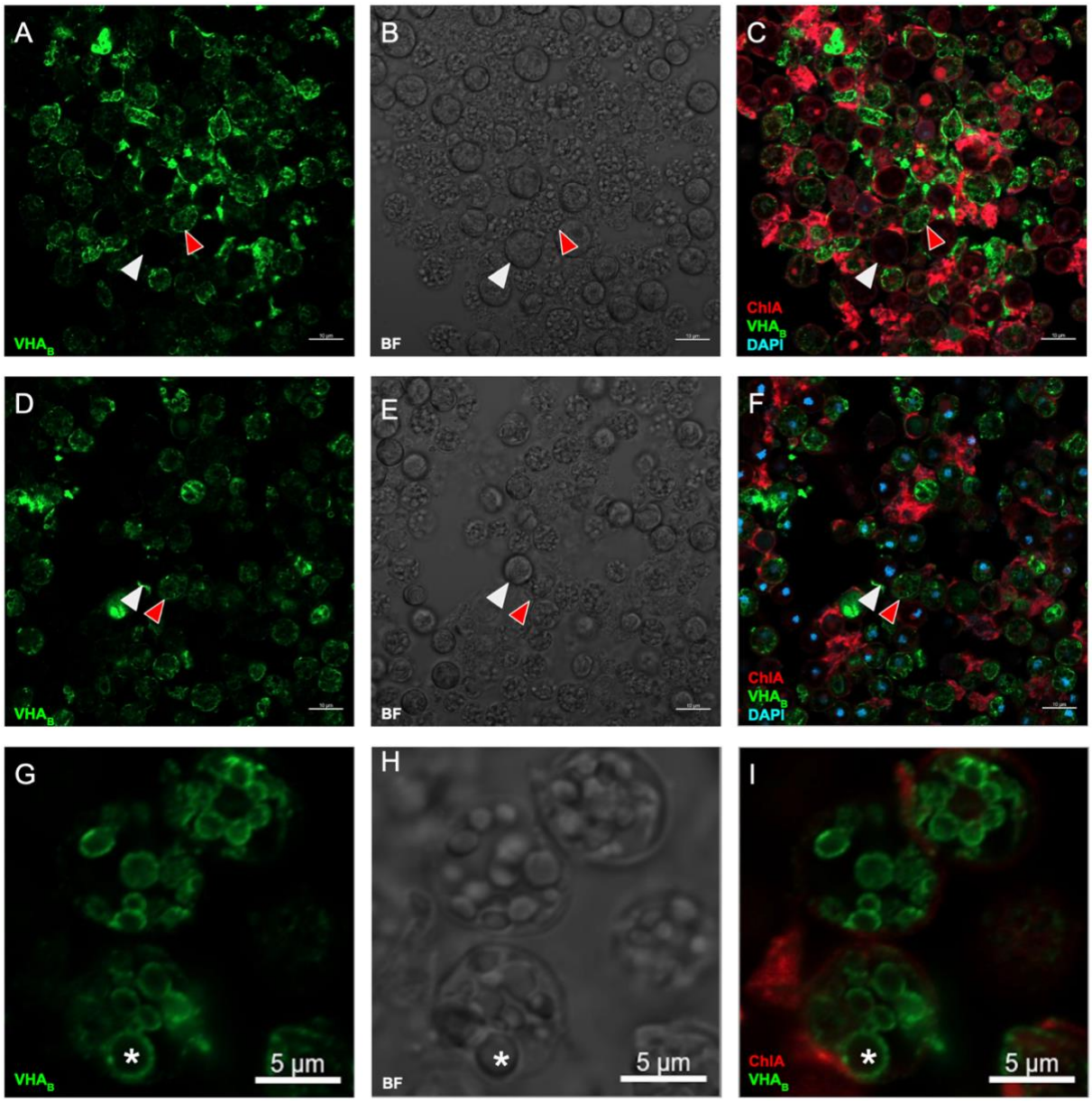

Figure 8. Immunofluorescent localization of VHA$_B$ in *M. leei* cells. (A) VHA$_B$ fluorescence in LL *M. leei* showing the difference between the sectioned (red arrow) and unsectioned cell (white arrow). (B) Bright field image showing the corresponding distinct appearance of the sectioned (red arrow) and unsectioned cell (white arrow). (C) Merged image showing chlorophyll A, VHA$_B$ and DAPI channels. (D) VHA$_B$ fluorescence in HL *M. leei* showing the difference between the sectioned (red arrow) and unsectioned cell (white arrow). (E) Bright field image showing the corresponding distinct appearance of the sectioned (red arrow) and unsectioned cell (white arrow). (F) Merged image showing chlorophyll A, VHA$_B$ and DAPI channels. (G) High magnification image showing VHA$_B$ fluorescence in HL *M. leei* with a close-up view of the spherical structure surrounded by VHA$_B$ signals (*). (I) Bright field image with (*) highlighting the cellular morphology without fluorescent labeling. (I) Merged image showing chlorophyll A and VHA$_B$. ChlA: chlorophyll A. BF: Bright field.

M. leei cells typically have one reticulate chloroplast on the periphery (Pochon & LaJeunesse, 2021). Chemical fixation slightly altered the shape of the chloroplast represented by chlorophyll A signals (visualized taking advantage of its far-red fluorescence) due to the cross-linking effect of PFA (Figure 9A & 9D). Analysis of bright field and fluorescent images revealed that VHA_B immunostaining often surrounded cell structures resembling vacuoles or chloroplasts (Figure 8). However, the use of organic solvents during ICC, which extracted chlorophyll pigments, prevented verification of these structures as chloroplasts (Figures 8C, 8F, and 8I). To overcome this limitation, I imaged the cells before and after fixation (but before exposing the cells to organic solvents). This approach allowed me to determine that chlorophyll A was not located inside the spherical structures (identified using bright field images) (Figure 9 D-F). A comparison between Figure 8 (G and H) and Figure 9 (D and E) indicates that VHA_B did not surround the chloroplast. This VHA_B subcellular localization is inconsistent with the colocalization of VHA_B with chloroplasts observed in *Thalassiosira pseudonana* (Yee et al., 2023). However, Yee et al. (2020) also noted VHA_B surrounding and acidifying vacuoles in the same species, and these vacuoles are important for providing buoyancy and storing nutrients for the algae. Similarly, maize root cells display VHA signals colocalizing with the endoplasmic reticulum and tonoplasts (Kluge et al., 2004). VHA in plant vacuoles is known to play a role in many physiological processes including metabolic regulation, signal transduction and sort and deliver processed membrane proteins when residing on endomembranes (reviewed by Sze et al., 1992). Future studies could co-stain VHA with vacuolar and endoplasmic reticulum polypeptide markers in Symbiodiniaceae to see if they co-localize and examine the potential role of VHA in other processes.

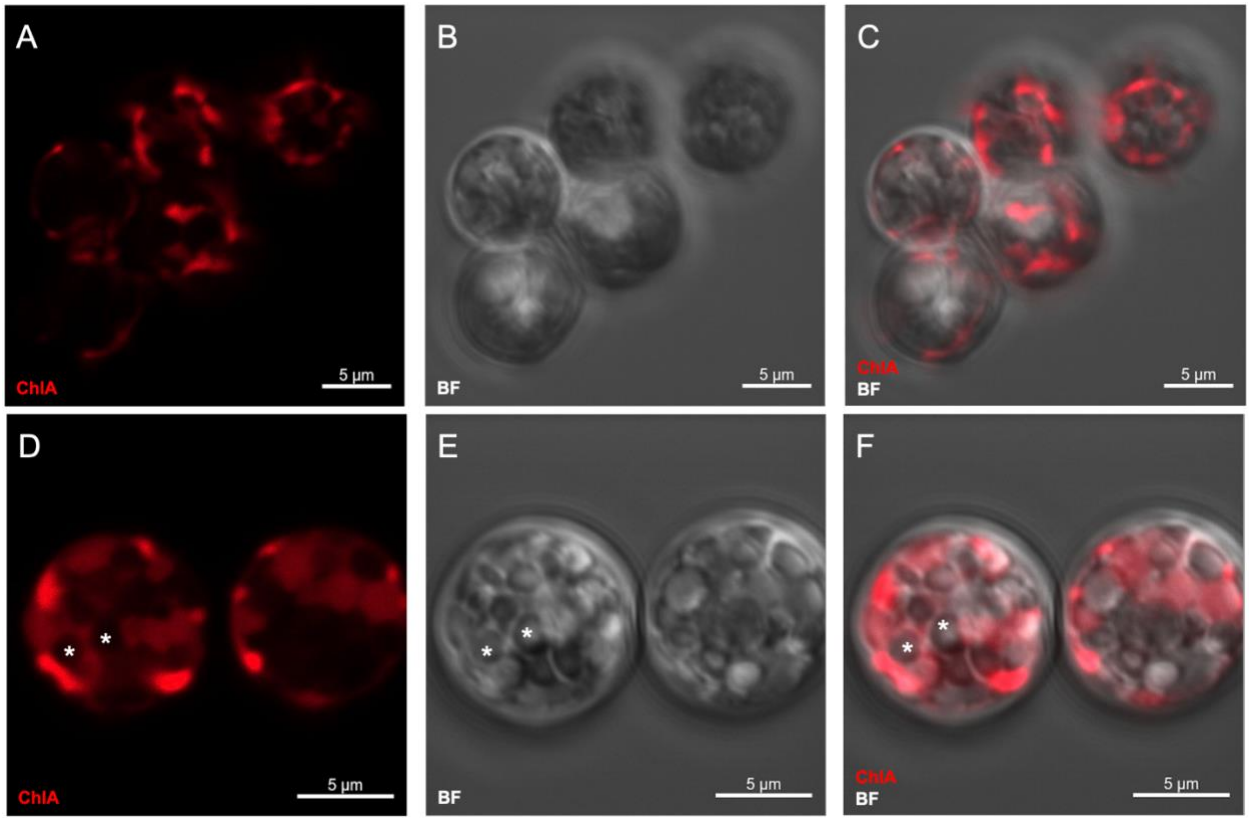

Figure 9. Chloroplast and vacuole-like structures in live and fixed *M. leei* cells. (A-C) Live cells. (A) Chlorophyll A fluorescence. (B) Bright field image. (C) Merged images showing chlorophyll A and bright field channels. (D-F) Fixed cells. (D) Chlorophyll A fluorescence; asterisks (*) mark the locations of spherical structures within the cells. (E) Bright field image with asterisks (*) corresponding to those identified in (D). (F) Merged images showing chlorophyll A and bright field channels. ChlA: chlorophyll A. BF:Bright field.

CONCLUSION AND FUTURE DIRECTIONS

My thesis is the first to examine the role of VHA in the CCM of the Symbiodiniaceae algae *B. psygmophilum* and *M. leei* through conducting functional experiments using a respirometry system and investigating VHA's subcellular localization using immunocytochemistry. Respirometry data show that inhibition of VHA using 100 nM ConcA in *B. psygmophilum* decreased O_2 production by ~ 20% when the cultures were illuminated by the light level they were acclimated to, indicating that VHA-mediated CCM may exist under these conditions. This percentage is similar to what Yee et al (2023) observed in the two diatoms, one type of dinoflagellates and one type of coccolithophores, which are all secondary endosymbiotic algae. However, Yee et al (2023) 10 nM ConcA while I used 100 nM, which might be due to differences in cell wall compositions that affect drug permeability among different types of algae. Given that the effect of ConcA and EZ on the O_2 production in *B. psygmophilum* varied greatly in this experiment, I suggest that future researchers carefully design the experiment, especially when choosing the light level and drug incubation time. It is also important to maintain consistency in the timing of conducting the experiment and use cultures at the same growth phase to minimize variations in algal circadian rhythm and cell growth phase. To further elucidate components in the CCM in Symbiodiniaceae, future researchers could utilize multi-omics approaches which help identify genes and proteins responsible for regulating CCM coupled with functional experiments and subcellular localization information.

My attempts to chemically fix *B. psygmophilum* were unsuccessful, necessitating alternative fixation approaches such as cryofixation. This method involves rapidly high-pressure freezing, which helps to preserve cellular structures without the introduction of potentially disruptive chemicals. Another option is expressing GFP-tagged VHA in live cells, which does not

require fixation. Future researchers can experiment these approaches on *B. psygmophilum* and proceed with ICC to examine protein subcellular localizations. My examination of VHA in *M. leei* revealed that VHA in *M. leei* did not localize around the chloroplasts but instead surrounded spherical vacuole-like structures within the cells. VHA in these vacuoles might be contributing to other processes in the algae such as buoyancy regulation, nutrients storage and processed protein delivery. To confirm the identity of the spherical structures, future researchers can co-stain membrane proteins with VHA. The differential morphological responses to fixatives between *B. psygmophilum* and *M. leei* revealed differences in their cell wall compositions and reaffirmed the diversity within the Symbiodiniaceae family.

I also confirmed that the gene PMA was symbiosis-dependent by comparing gene expression between symbiotic algae in *Stylophora pistillata* and cultured *B. psygmophilum*. Additionally, symbiotic and free-living algae exhibit many differences: symbiotic algae grow slower than free-living algae, lack flagella that enable mobility, and differentially expressed a variety of genes (Davy et al., 2012; Wooldridge, 2010; Maor-Landaw et al., 2020). Understanding these differences is crucial for predicting how sensitive the symbiosis is to climate change: whether establishing a symbiotic relationship remains ideal to both the symbiont and the host under environmental stressors. It is important to note that the culture medium used in this project, ASP-8A+α, does not reflect the oligotrophic environments where corals and free-living algae typically inhabit, thus limiting its applicability in simulating real-world conditions (Maruyama & Weis, 2021). While this project has provided valuable insights into the morphology and physiology of these algae, these findings might not fully represent their natural state in seawater. Future research should carefully consider the impact of culture media on experimental outcomes.

In this project, I observed great morphological and physiological differences between the two Symbiodiniaceae species. *B. psygmophilum* possesses cup-shaped chloroplasts, while *M. leei* have one single reticulate chloroplast. And *B. psygmophilum* grew much faster than *M. leei* in the laboratory condition. Further investigation into variations within the Symbiodiniaceae family can inform the selective advantages of these variations in establishing their unique symbiotic relationships. Understanding these variations can also help predict how these algae will respond to environmental stressors and whether they could survive in the face of climate changes. This information can help develop targeted conservation strategies which include selecting resilient seeding species for restoration projects.

APPENDIX

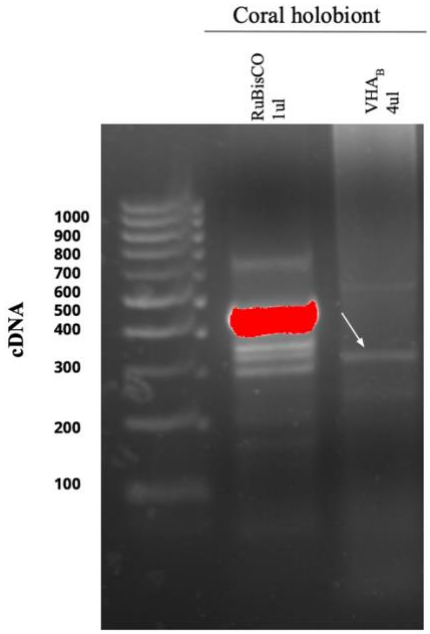

Supplemental Figure 1. PCR of VHA cDNA from coral holobiont. 1ul of cDNA was added to the reaction using the RuBisCO primers and 4ul of cDNA was added to the reaction using VHA primers. The band indicated by the white arrow was excised and sequenced.

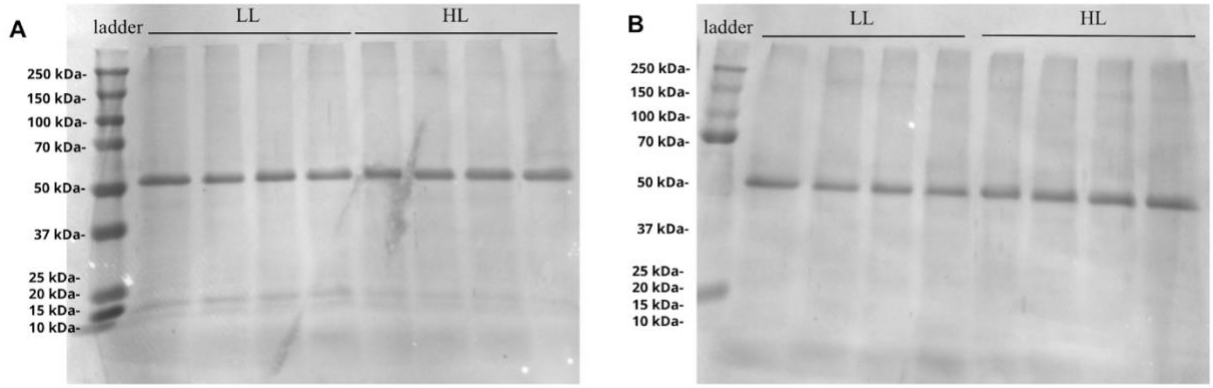

Supplemental Figure 2. Coomassie stained western blot membranes shown in Figure 3 A & C. (A) The membrane that is standardized by cell number (B) The membrane that is standardized by protein concentration.

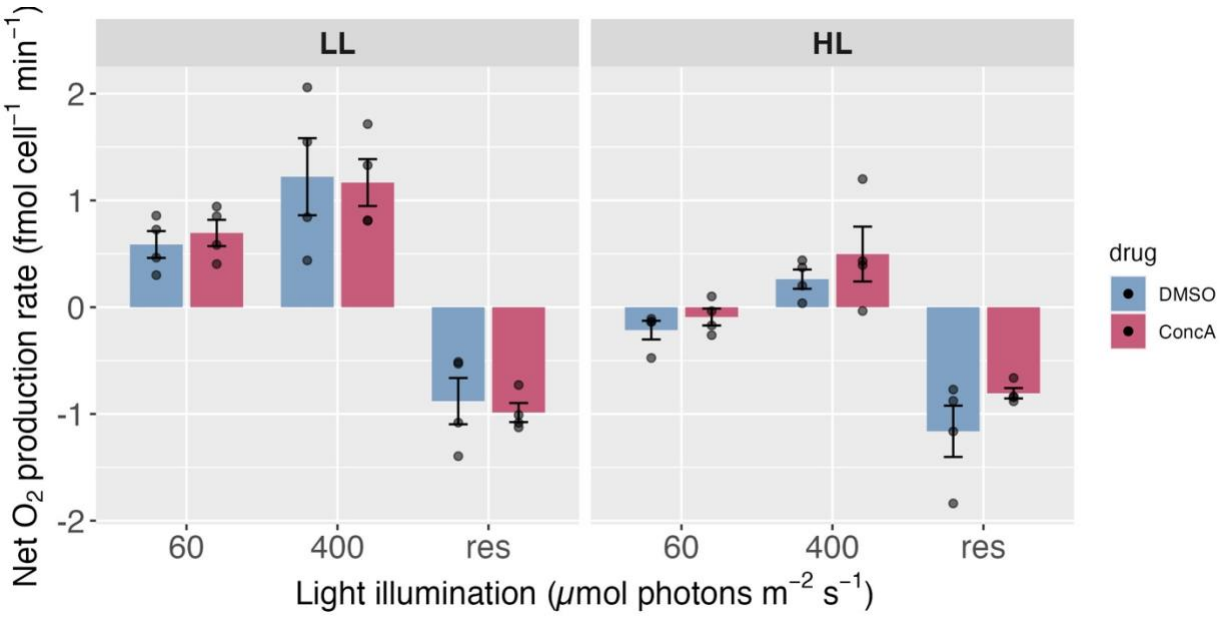

Supplemental Figure 3. O_2 production of LL (N=4) and HL (N=4) *B. psygmophilum* cultures after 2 h dark incubation in DMSO or 10 nM ConcA. res: dark.

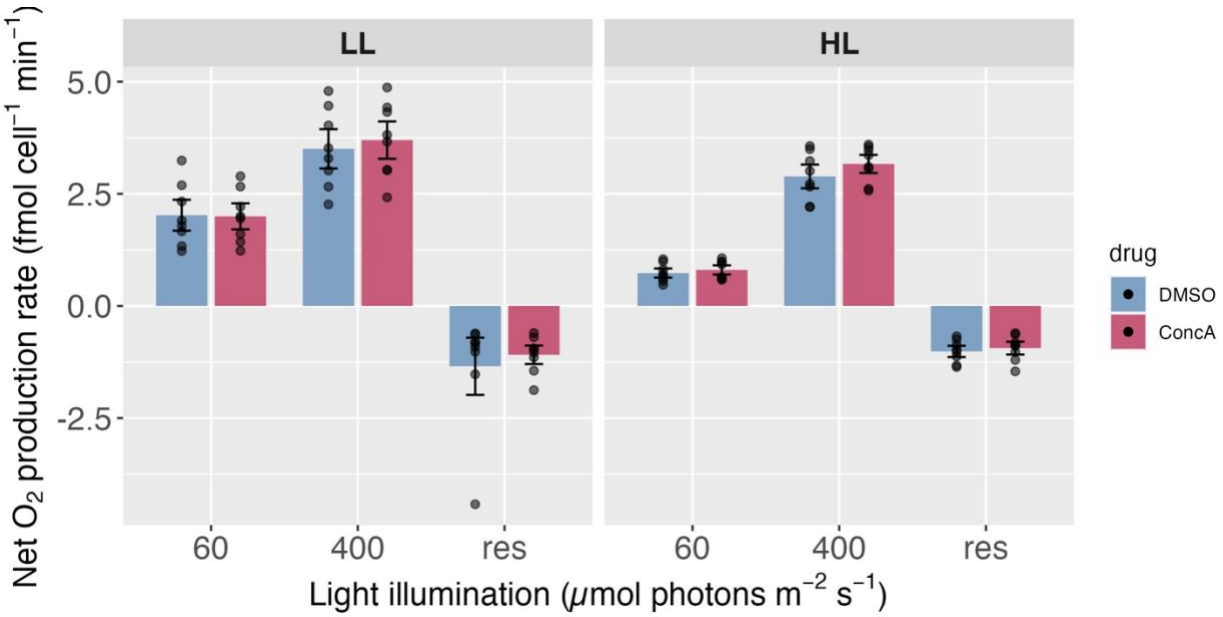

Supplemental Figure 4. O_2 production of LL (N=8) and HL (N=8) *B. psygmophilum* cultures after 2 h dark incubation in DMSO or 50 nM ConcA. res: dark.

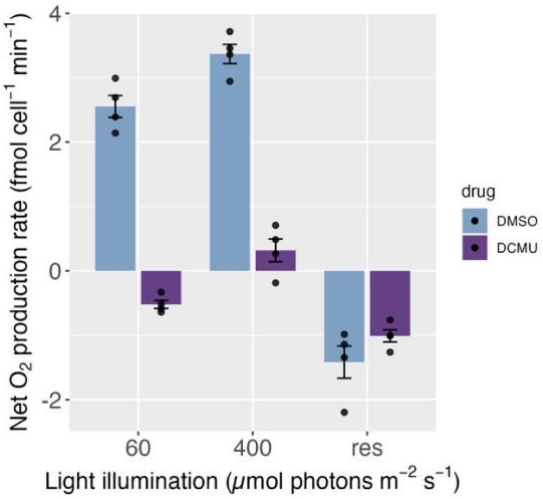

Supplemental Figure 5. O_2 production of LL (N=4) *B. psygmophilum* cultures after 10 min dark incubation in DMSO or 10 µM DCMU. res: dark.

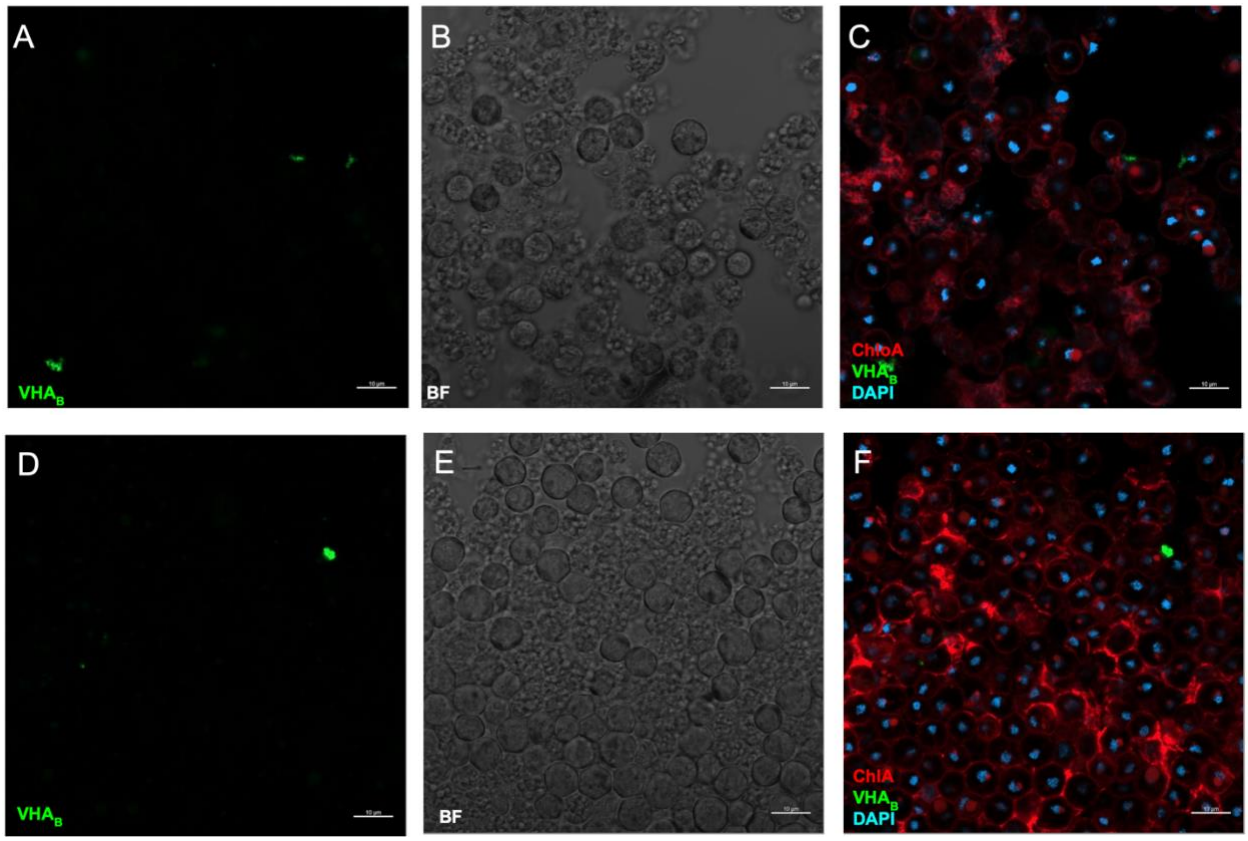

Supplemental Figure 6. Low magnification confocal images of no-primary-antibody PBS control *M. leei* cells. (A-C) LL *M. leei* cells. (D-F) HL *M. leei* cells.

REFERENCES

Abrego, David, Madeleine JH Van Oppen, and Bette L. Willis. "Highly infectious symbiont dominates initial uptake in coral juveniles." Molecular ecology 18, no. 16 (2009): 3518-3531.

Andrews, T. John, and George H. Lorimer. "Rubisco: structure, mechanisms, and prospects for improvement." *Photosynthesis*. Academic Press, 1987. 131-218.

Armstrong, Eric J., Jinae N. Roa, Jonathon H. Stillman, and Martin Tresguerres. "Symbiont photosynthesis in giant clams is promoted by V-type H^+-ATPase from host cells." J*ournal of Experimental Biology* 221, no. 18 (2018): jeb177220.

Baird, Andrew H., James R. Guest, and Bette L. Willis. "Systematic and biogeographical patterns in the reproductive biology of scleractinian corals." *Annual Review of Ecology, Evolution, and Systematics* 40, no. 1 (2009): 551-571.

Barott, Katie L., Alexander A. Venn, Sidney O. Perez, Sylvie Tambutté, and Martin Tresguerres. "Coral host cells acidify symbiotic algal microenvironment to promote photosynthesis." *Proceedings of the National Academy of Sciences* 112, no. 2 (2015): 607-612.

Barott, Katie L., Angus B. Thies, and Martin Tresguerres. "V-type H+-ATPase in the symbiosome membrane is a conserved mechanism for host control of photosynthesis in anthozoan photosymbioses." *Royal Society Open Science* 9, no. 1 (2022): 211449.

Baumgarten, Sebastian, Till Bayer, Manuel Aranda, Yi Jin Liew, Adrian Carr, Gos Micklem, and Christian R. Voolstra. "Integrating microRNA and mRNA expression profiling in *Symbiodinium microadriaticum*, a dinoflagellate symbiont of reef-building corals." *BMC genomics* 14 (2013): 1-18.

Bertucci, Anthony, Éric Tambutté, Sylvie Tambutté, Denis Allemand, and Didier Zoccola. "Symbiosis-dependent gene expression in coral–dinoflagellate association: cloning and characterization of a P-type H+-ATPase gene." *Proceedings of the Royal Society B: Biological Sciences* 277, no. 1678 (2010): 87-95.

Canfield, Donald Eugene. "The early history of atmospheric oxygen: homage to Robert M. Garrels." *Annu. Rev. Earth Planet. Sci*. 33 (2005): 1-36.

Castillo-Medina, Raúl E., Georgina Arzápalo-Castañeda, and Marco A. Villanueva. "Making walled-, highly autofluorescent dinoflagellate algae cells accessible and amenable for immunofluorescence and application of fluorescent probes." *Limnology and Oceanography: Methods* 9, no. 10 (2011): 460-465.

Cecchin, Michela, Jovan Simicevic, Louise Chaput, Manuel Hernandez Gil, Laura Girolomoni, Stefano Cazzaniga, Claire Remacle, Julia Hoeng, Nikolai V Ivanov, Bjoern Titz and Matteo Ballottari. "Acclimation strategies of the green alga *Chlorella vulgaris* to different light regimes revealed by physiological and comparative proteomic analyses." *Journal of Experimental Botany* 74, no. 15 (2023): 4540-4558.

Couso, Inmaculada, María Esther Pérez-Pérez, Enrique Martínez-Force, Hee-Sik Kim, Yonghua He, James G. Umen, and José L. Crespo. "Autophagic flux is required for the synthesis of triacylglycerols and ribosomal protein turnover in *Chlamydomonas*." *Journal of Experimental Botany* 69, no. 6 (2018): 1355-1367.

Davy, Simon K., Denis Allemand, and Virginia M. Weis. "Cell biology of cnidarian-dinoflagellate symbiosis." *Microbiology and Molecular Biology Reviews* 76, no. 2 (2012): 229-261.

Di, Anke, Mary E. Brown, Ludmila V. Deriy, Chunying Li, Frances L. Szeto, Yimei Chen, Ping Huang, Jiankun Tong, Anjaparavanda P. Naren, Vytautas Bindokas, H. Clive Palfrey and Deborah J. Nelson. "CFTR regulates phagosome acidification in macrophages and alters bactericidal activity." *Nature cell biology* 8, no. 9 (2006): 933-944.

Dong, Hong-Po, Yue-Lei Dong, Lei Cui, Srinivasan Balamurugan, Jian Gao, Song-Hui Lu, and Tao Jiang. "High light stress triggers distinct proteomic responses in the marine diatom *Thalassiosira pseudonana*." *BMC genomics* 17 (2016): 1-14.

Forgac, Michael. "Vacuolar ATPases: rotary proton pumps in physiology and pathophysiology." *Nature reviews Molecular cell biology* 8, no. 11 (2007): 917-929.

Fujise, Lisa, David J. Suggett, Michael Stat, Tim Kahlke, Michael Bunce, Stephanie G. Gardner, Samantha Goyen, Stephen Woodcock, Peter J. Ralph, Justin R. Seymour, Nachshon Siboni and Matthew R. Nitschke. "Unlocking the phylogenetic diversity, primary habitats, and abundances of free-living Symbiodiniaceae on a coral reef." *Molecular Ecology* 30, no. 1 (2021): 343-360.

Harrison, Peter Lynton, and Carden C. Wallace. "Reproduction, dispersal and recruitment of scleractinian corals." *In Coral reefs*, vol. 25, pp. 133-207. Elsevier, 1990.

Iglesias-Prieto, Roberto, and Robert K. Trench. "Acclimation and adaptation to irradiance in symbiotic dinoflagellates. I. Responses of the photosynthetic unit to changes in photon flux density." *Marine ecology progress series*. Oldendorf 113, no. 1 (1994): 163-175.

Jeong, Hae Jin, Yeong Du Yoo, Nam Seon Kang, An Suk Lim, Kyeong Ah Seong, Sung Yeon Lee, Moo Joon Lee, Kyung Ha Lee, Hyung Seop Kim, Woongghi Shin, Seung Won Nam, Wonho Yih, Kitack Lee. "Heterotrophic feeding as a newly identified survival strategy of the dinoflagellate *Symbiodinium*." *Proceedings of the National Academy of Sciences* 109, no. 31 (2012): 12604-12609.

Kluge, Christoph, Thorsten Seidel, Susanne Bolte, Shanti S. Sharma, Miriam Hanitzsch, Beatrice Satiat-Jeunemaitre, Joachim Roß, Markus Sauer, Dortje Golldack, and Karl-Josef Dietz. "Subcellular distribution of the V-ATPase complex in plant cells, and in vivo localisation of the 100 kDa subunit VHA-a within the complex." *BMC Cell Biology* 5 (2004): 1-18.

Kwok, Alvin Chun Man, Wai Sun Chan, and Joseph Tin Yum Wong. "Dinoflagellate amphiesmal dynamics: Cell wall deposition with ecdysis and cellular growth." *Marine Drugs* 21, no. 2 (2023): 70.

LaJeunesse, Todd C., John Everett Parkinson, Paul W. Gabrielson, Hae Jin Jeong, James Davis Reimer, Christian R. Voolstra, and Scott R. Santos. "Systematic revision of Symbiodiniaceae highlights the antiquity and diversity of coral endosymbionts." *Current Biology* 28, no. 16 (2018): 2570-2580.

LaJeunesse, T. J. M. B. "Diversity and community structure of symbiotic dinoflagellates from Caribbean coral reefs." *Marine biology* 141 (2002): 387-400.

Lee, John J., and Pamela Hallock. "Algal symbiosis as the driving force in the evolution of larger foraminifera a." *Annals of the New York Academy of Sciences* 503, no. 1 (1987): 330-347.

Lee, Robert Edward. "Evolution of algal flagellates with chloroplast endoplasmic reticulum from the ciliates." *South African Journal of Science* 73, no. 6 (1977): 179.

Lee, Robert Edward, and Paul Kugrens. "Hypothesis: the ecological advantage of chloroplast ER–the ability to outcompete at low dissolved CO2 concentrations." *Protist* 149, no. 4 (1998): 341-345.

Lee, Robert Edward, and Paul Kugrens. "Ancient atmospheric CO2 and the timing of evolution of secondary endosymbioses." *Phycologia* 39, no. 2 (2000): 167-172.

Liu, Yansheng, Andreas Beyer, and Ruedi Aebersold. "On the dependency of cellular protein levels on mRNA abundance." *Cell* 165, no. 3 (2016): 535-550.

Maor-Landaw, Keren, Madeleine JH van Oppen, and Geoffrey I. McFadden. "Symbiotic lifestyle triggers drastic changes in the gene expression of the algal endosymbiont *Breviolum minutum* (Symbiodiniaceae)." *Ecology and Evolution* 10, no. 1 (2020): 451-466.

MARKELL, DOUGLAS A., ROBERT K. TRENCH, and Roberto Iglesias-Prieto. "Macromolecules associated with the cell walls of symbiotic dinoflagellates." *Symbiosis* (1992).

Maruyama, Shumpei, and Virginia M. Weis. "Limitations of using cultured algae to study cnidarian-algal symbioses and suggestions for future studies." *Journal of Phycology* 57, no. 1 (2021): 30-38.

McFadden, Geoffrey Ian. "Primary and secondary endosymbiosis and the origin of plastids." *Journal of Phycology* 37, no. 6 (2001): 951-959.

McLaughlin, J. J. A., and P. A. Zahl. "Endozoic algae." *Symbiosis* 1 (1966): 257-297.

Moroney, James V., H. David Husic, and N. E. Tolbert. "Effect of carbonic anhydrase inhibitors on inorganic carbon accumulation by *Chlamydomonas reinhardtii*." *Plant Physiology* 79, no. 1 (1985): 177-183.

Muscatine, L., P. G. Falkowski, J. W.Porter, and Z. Dubinsky. "Fate of photosynthetic fixed carbon in light-and shade-adapted colonies of the symbiotic coral *Stylophora pistillata*." *Proceedings of the Royal Society of London. Series B. Biological Sciences* 222, no. 1227 (1984): 181-202.

Muscatine, L. (1990). "The role of symbiotic algae in carbon and energy flux in reef corals." *Ecosystems of the World* 25: 75-87.

Obiol, Aleix, David López-Escardó, Eric D. Salomaki, Monika M. Wiśniewska, Irene Forn, Elisabet Sà, Dolors Vaqué, Martin Kolísko, and Ramon Massana. "Gene expression dynamics of natural assemblages of heterotrophic flagellates during bacterivory." *Microbiome* 11, no. 1 (2023): 134.

Palmgren, Michael G. "Plant plasma membrane H+-ATPases: powerhouses for nutrient uptake." *Annual review of plant biology* 52, no. 1 (2001): 817-845.

Pawlowski, J. A. N., MARIA HOLZMANN, JOSÉ F. FAHRNI, XAVIER POCHON, and JOHN J. LEE. "Molecular identification of algal endosymbionts in large miliolid foraminifera: 2. Dinoflagellates." *Journal of Eukaryotic Microbiology* 48, no. 3 (2001): 368-373.

Pochon, Xavier, and Todd C. LaJeunesse. "Miliolidium n. gen, a new symbiodiniacean genus whose members associate with soritid foraminifera or are free-living." *Journal of Eukaryotic Microbiology* 68, no. 4 (2021): e12856.

Pronina, Natalia A., and Victor E. Semenenko. "Membrane-bound carbonic anhydrase takes part in CO_2 concentration in algae cells." *In Current Research in Photosynthesis: Proceedings of the VIIIth International Conference on Photosynthesis Stockholm, Sweden, August 6–11, 1989*, pp. 3283-3286. Dordrecht: Springer Netherlands, 1990.

Pronina, N. A., Z. M. Ramazanov, and V. E. Semenenko. "Carbonic anhydrase activity of Chlorella cells as a function of CO2 concentration." *Soviet plant physiology* (1981).

Robison, Jennifer D., and Mark E. Warner. "Differential impacts of photoacclimation and thermal stress on the photobiology of four different phylotypes of *Symbiodinium* (pyrrhophyta) 1." *Journal of phycology* 42, no. 3 (2006): 568-579.

Rosic, Nedeljka, Edmund Yew Siang Ling, Chon-Kit Kenneth Chan, Hong Ching Lee, Paulina Kaniewska, David Edwards, Sophie Dove, and Ove Hoegh-Guldberg. "Unfolding the secrets of coral–algal symbiosis." *The ISME journal* 9, no. 4 (2015): 844-856.

Sze, Heven, John M. Ward, and Shoupeng Lai. "Vacuolar H^+-translocating ATPases from plants: structure, function, and isoforms." *Journal of bioenergetics and biomembranes* 24 (1992): 371-381.

Takabayashi, M., L. M. Adams, X. Pochon, and R. D. Gates. "Genetic diversity of free-living *Symbiodinium* in surface water and sediment of Hawai ‘i and Florida." *Coral Reefs* 31 (2012): 157-167.

Thies, Angus B., Alex R. Quijada-Rodriguez, Haonan Zhouyao, Dirk Weihrauch, and Martin Tresguerres. "A Rhesus channel in the coral symbiosome membrane suggests a novel mechanism to regulate NH_3 and CO_2 delivery to algal symbionts." *Science advances* 8, no. 10 (2022): eabm0303.

Tortorelli, Giada, Clinton A. Oakley, Simon K. Davy, Madeleine JH van Oppen, and Geoffrey I. McFadden. "Cell wall proteomic analysis of the cnidarian photosymbionts *Breviolum minutum* and *Cladocopium goreaui*." *Journal of Eukaryotic Microbiology* 69, no. 1 (2022): e12870.

Trench, R. K. "The cell biology of plant-animal symbiosis." *Annual Review of Plant Physiology* 30, no. 1 (1979): 485-531.

Trench, R. (1993). "Microalgal-invertebrate symbiosis, a review." *Endocytobiosis* Cell Res 9: 135-175.

Trench, R. K. (1987). "Dinoflagellates in non-parasitic symbioses." *The biology of dinoflagellates*: 530-570.

Wakefield, Timothy S., Mark A. Farmer, and Stephen C. Kempf. "Revised description of the fine structure of *in situ*" zooxanthellae" genus *Symbiodinium*." *The Biological Bulletin* 199, no. 1 (2000): 76-84.

Wang, Zhong, Mark Gerstein, and Michael Snyder. "RNA-Seq: a revolutionary tool for transcriptomics." *Nature reviews genetics* 10, no. 1 (2009): 57-63.

Wooldridge, Scott A. "Is the coral-algae symbiosis really ‘mutually beneficial’ for the partners?." *BioEssays* 32, no. 7 (2010): 615-625.

Yee, Daniel P., Mark Hildebrand, and Martin Tresguerres. "Dynamic subcellular translocation of V-type H^+-ATPase is essential for biomineralization of the diatom silica cell wall." *New Phytologist* 225, no. 6 (2020): 2411-2422.

Yee, Daniel P., Ty J. Samo, Raffaela M. Abbriano, Bethany Shimasaki, Maria Vernet, Xavier Mayali, Peter K. Weber, B. Greg Mitchell, Mark Hilderbrand, Johan Decelle, and Martin Tresguerres. "The V-type ATPase enhances photosynthesis in marine phytoplankton and further links phagocytosis to symbiogenesis." *Current Biology* 33, no. 12 (2023): 2541-2547.

Zeng, Xiaopeng, Peng Jin, Jianrong Xia, and Yuxian Liu. "Correlation of carbonic anhydrase and Rubisco in the growth and photosynthesis in the diatom *Phaeodactylum tricornutum*." *Journal of Applied Phycology* 31 (2019): 123-129.

Zhang, Huiying, Rensen Zeng, Daoyi Chen, and Jian Liu. "A pivotal role of vacuolar H+-ATPase in regulation of lipid production in *Phaeodactylum tricornutum*." *Scientific reports* 6, no. 1 (2016): 31319.